Special issue review article

NMR IN BIOMEDICINE

Received: 27 March 2015, Revised: 9 November 2015, Accepted: 12 November 2015, Published online in Wiley Online Library: 15 January 2016

(wileyonlinelibrary.com) DOI: 10.1002/nbm.3458

Diffusion MRI in early cancer therapeutic response assessment

C. J. Galbán, B. A. Hoff, T. L. Chenevert and B. D. Ross*

Imaging biomarkers for the predictive assessment of treatment response in patients with cancer earlier than standard tumor volumetric metrics would provide new opportunities to individualize therapy. Diffusion-weighted MRI (DW-MRI), highly sensitive to microenvironmental alterations at the cellular level, has been evaluated extensively as a technique for the generation of quantitative and early imaging biomarkers of therapeutic response and clinical outcome. First demonstrated in a rodent tumor model, subsequent studies have shown that DW-MRI can be applied to many different solid tumors for the detection of changes in cellularity as measured indirectly by an increase in the apparent diffusion coefficient (ADC) of water molecules within the lesion. The introduction of quantitative DW-MRI into the treatment management of patients with cancer may aid physicians to individualize therapy, thereby minimizing unnecessary systemic toxicity associated with ineffective therapies, saving valuable time, reducing patient care costs and ultimately improving clinical outcome. This review covers the theoretical basis behind the application of DW-MRI to monitor therapeutic response in cancer, the analytical techniques used and the results obtained from various clinical studies that have demonstrated the efficacy of DW-MRI for the prediction of cancer treatment response. Copyright © 2016 John Wiley & Sons, Ltd.

Keywords: review article; cancer treatment response; imaging biomarker; functional diffusion map; diffusion-weighted MRI

INTRODUCTION

Monitoring cancer treatment response

Image-based assessment of cancer treatment response continues to be an active area of research with advances in medical imaging instrumentation providing opportunities to fundamentally change the clinical management of patients with cancer. MRI represents a key modality that has found use in the diagnosis, treatment planning, and assessment of response and recurrence of solid malignancies. By providing high spatial resolution and soft tissue contrast, MRI allows exquisite noninvasive radiographic detection of tumor location, whilst also providing a determination of the tumor number and dimensions.

Computed tomography and, soon after, MRI have been used since the 1960s to measure gross changes in tumor volume following a therapeutic intervention (1). Although there have been advancements in quantitative imaging techniques, such as diffusion-weighted MRI (DW-MRI), dynamic contrast-enhanced MRI (DCE-MRI) and fluorodeoxyglucose-positron emission tomography (FDG-PET), standard practice for patient management and clinical trials continues to employ anatomical images to assess tumor response to treatment (2–4). The World Health Organization (WHO) and the Response Evaluation Criteria in Solid Tumors (RECIST) have proposed guidelines primarily based on a single linear summation of specific lesions, where monitoring of the morphological changes in tumor volume allows for routine measurements for cancer response assessment. Nevertheless, there continues to be growing concerns regarding the adequacy of these criteria as some treatments, such as molecularly targeted agents, may provide therapeutic benefit without significantly reducing the tumor volume (5–7). These concerns underscore the urgency for the development and implementation of reliable response imaging biomarkers or surrogates that can detect response to treatment earlier than current methodologies (8,9).

GENERAL CONCEPTS IN DIFFUSION

The first diffusion MR sequence was demonstrated in 1965 by Stejskal and Tanner (10) and, by the 1980s, DW-MRI of *in vivo* systems was reported (11–13). Since then, reviews have been generated on the principles and technical aspects of this MR technique, as well as consensus recommendations using diffusion imaging as a response metric for treatment assessment (14–16). Molecular diffusion is the thermally driven random translational motion of molecules in media, which is referred to as 'Brownian motion'. Key factors that exert their influence on the mobility of a diffusing molecule include medium viscosity, temperature and its molecular mass. Diffusion is not a magnetization-related process such as, for example, T_1 and T_2

* *Correspondence to: B. D. Ross, University of Michigan School of Medicine, Center for Molecular Imaging and Department of Radiology, Biomedical Sciences Research Building, 109 Zina Pitcher Place, Ann Arbor, MI 48109, USA. E-mail: bdross@umich.edu*

C. J. Galbán, B. A. Hoff, T. L. Chenevert, B. D. Ross
Department of Radiology, Center for Molecular Imaging, University of Michigan, Ann Arbor, MI, USA

Abbreviations used: *ADC, apparent diffusion coefficient; CR, complete response; DCE-MRI, dynamic contrast-enhanced MRI; DW-MRI, diffusion-weighted MRI; EPI, echo-planar imaging; FDG-PET, fluorodeoxyglucose-positron emission tomography; FDM, functional diffusion map; HNSCC, head and neck squamous cell carcinoma; NAC, neoadjuvant chemotherapy; PCR, pathological complete response; PR, partial response; PRM, parametric response mapping; RECIST, Response Evaluation Criteria in Solid Tumors; Tc99m-SPECT, technetium 99m single photon emission computed tomography; wbDW-MRI, whole-body diffusion-weighted MRI; WHO, World Health Organization.*

magnetization relaxation, which drives conventional MRI contrast. Nevertheless, MRI can be used to noninvasively quantify (image) water diffusion values spatially *in vivo*. This is accomplished in part through the use of magnetic gradients that allow for the 'encoding' of initial locations of constituent water molecules in the tissue. Following a brief interval, the same gradients are used to 'decode' the molecular locations. For those water molecules in which displacement has occurred during the time interval, decoding will be incomplete, resulting in the loss of signal through spin dephasing. The dephasing amount increases in proportion to the distance translated between encode/decode diffusion gradient pulses. Highly mobile water molecules will have greater attenuation of the signal relative to water in more restricted/cellular tissue environments. The determination of the degree of signal loss at various diffusion gradient settings provides for the ability to calculate molecular mobility in complex systems, such as tumor tissue. However, because tumor tissue is composed of water located in a highly complex microenvironment, the concept of a single diffusion coefficient is not valid and, as such, it is reported as an 'apparent diffusion coefficient' (ADC) (13,14). ADC measurements can be used to assess a myriad of properties that impede molecular motions, including cell membrane integrity, cell density, interactions with macromolecules, and processes that enhance mobility via active transport, convective motion and perfusion.

The ability of water to sample its surrounding environment is the foundation behind its efficacy as a measure of tumor response to cancer. The thermal, i.e. Brownian, motion of free water at body temperature (~35 °C) is approximately 3×10^{-3} mm^2/s. Clinical DW-MRI sequences typically have a bipolar gradient interval around 50 ms, resulting in a displacement of free water molecules of 30 μm. By applying these motion-sensitive gradients, water molecules can be exploited to sample the microenvironment of biological systems well within the resolution of the MRI sequence. Structures within the solid tumor that are sampled by water molecules may include the tumor cell membranes, organelles, myelin layers and macromolecules, as well as additional cellular and subcellular entities, all of which are on the order of micrometers. Transient association of water with large, slow-moving macromolecules and cell membranes that result in water binding, as well as impediment by membranes and other structures, effectively reduce water mobility to an ADC lower than free water diffusion. The greater the bulk density of structures within a tumor tissue that impede water mobility, the lower the ADC value for that tumor. As such, ADC is considered to be a noninvasive imaging biomarker of cellularity or cell density. However, if two tissues have different ADC values, the lower ADC tissue may not necessarily have the greater number of cells per unit volume. Other factors that make up the microenvironment (e.g. cell size, viscosity, vasculature, extracellular matrix and permeability) also affect water mobility and ADC. Within a given tissue or cell type, ADC is useful as an indicator of the relative cellularity, such as in the evolution of a tumor over time following therapy. Cellular alterations caused by disease or intervention, as well as changes in cellular organization or integrity of cellular elements, are available for study by diffusion imaging.

Water diffusion on the order of cellular distances is measurable in spite of the presence of other much larger physiologic motions. A single-shot echo-planar imaging (EPI) approach (17) is the standard imaging sequence for the acquisition of diffusion-weighted imaging. By acquiring the entire set of echoes for an image within one single scanning period, respiratory bulk tissue motion, which would overwhelm the measurement of molecular motion, is essentially eliminated. By decreasing the acquisition times by a factor of 100, EPI also allows DW-MRI to be incorporated as a standard MRI sequence in clinical scanners to be used in routine clinical scanning protocols. However, images generated by EPI are sensitive to artifacts, such as distortion and signal loss owing to magnetic susceptibility. These limitations aside, EPI is the most commonly used clinical sequence, combined with diffusion sensitization gradient pulses, to perform DW-MRI.

ADC AS A MEASURE OF TUMOR CELLULARITY

It is traditionally viewed that, as cellular density increases, the added tortuosity within the microenvironment reduces water mobility. Figure 1 illustrates the effect of an effective therapeutic agent on the water diffusivity in a solid tumor mass (18). Solid tumors typically have a mean ADC value around 1×10^{-3} mm^2/s (Fig. 1). Following the intervention of a therapeutic agent that results in cell killing (i.e. a decrease in tumor cellularity), the extracellular space increases as the intracellular space diminishes (Fig. 1). This results in a shift in the tumor water diffusivity to higher values in therapeutically responsive regions of the tumor. Several groups have reported the inverse relationship between ADC and cellular density (19–22). To aid in the interpretation of these results, a biphasic model relating ADC values to cellularity has been proposed in which two pools of water within the tissue exist: a fast diffusion pool and a slow diffusion pool (23). The slow diffusion pool is proposed to consist of a water layer trapped by electrostatic forces of the cellular membranes and associated cytoskeleton. The fast diffusion pool is thought to belong to a combination of intra- and extracellular compartments which are, however, slower than free water. Both the traditional, i.e. monoexponential, and biphasic diffusion models provide for the rationale that water diffusion will decrease during cell swelling or cell proliferation, and increase during treatment-induced loss of cellular viability or density. Regardless of the underlying mechanism, the fact remains that tumor diffusion values increase as tumor tissue initially progresses from a solid, cellular lesion to an acellular, necrotic tumor during successful cytotoxic therapy. This characteristic of tumor water diffusion values provides a key opportunity to use this biophysical and quantifiable ADC parameter as a sensitive biomarker for the detection of the underlying changes in tumor cytoarchitecture associated with treatment (24).

DIFFUSION IMAGING TO ASSESS TREATMENT RESPONSE

Twenty years of research in preclinical studies have supported the notion that water diffusivity is highly dependent on the tumor microenvironment. This suggests that diffusion MR can be used to noninvasively detect cellular changes associated with treatment-induced cell killing in animal models (19,20,22,25–30). The key findings in many studies are that changes in ADC values precede changes in tumor volume regression, as well as being treatment independent and dose/efficacy dependent. All of this supports the claim that this imaging biomarker may indeed be used as an early surrogate for the assessment of treatment outcome.

Diffusion MRI as a method for therapeutic response assessment in the clinic was first demonstrated in patients with glioma (21). Tumors treated with radiation, with or without chemotherapy, demonstrated an increase in ADC values from baseline. The

NMR IN BIOMEDICINE

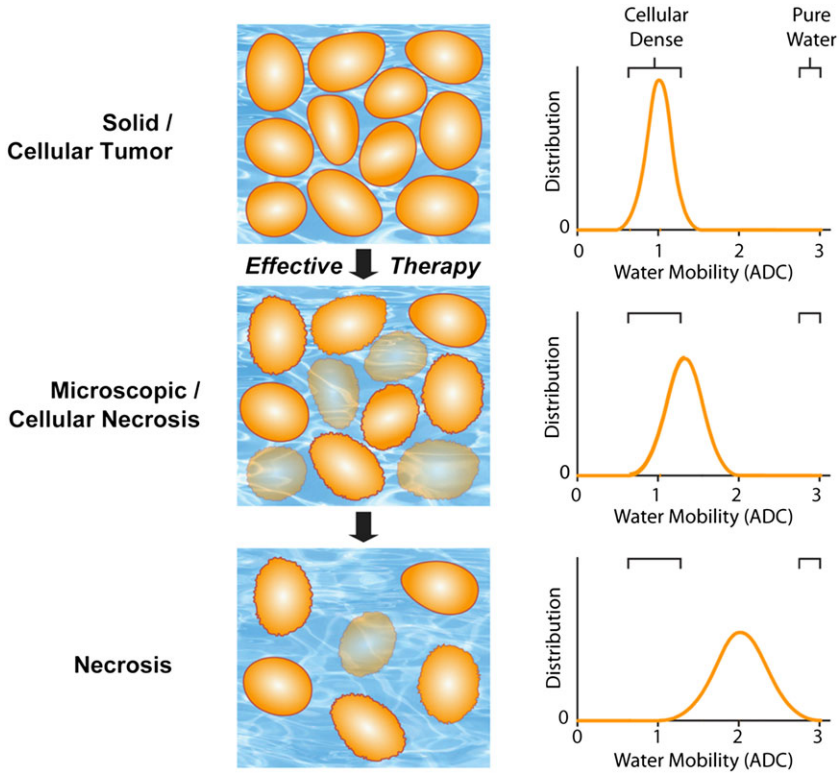

Figure 1. Schematic diagram of changes in water diffusivity in a tumor following an effective therapeutic agent. Changes in cellularity (left) occur with increasing molecular water mobility, measured as the apparent diffusion coefficient (ADC; right), as a tumor responds to treatment (top to bottom). As a tumor responds to therapy, an increase in extracellular space and membrane permeability occurs, which allows for increased water mobility, and is detected by diffusion-weighted MRI (DW-MRI) as an increase in ADC values. [Courtesy of ref. (18).]

magnitude of change in ADC values correlated with cellularity in the tumor mass, albeit in a pilot study. Through advances in radiofrequency coil design, parallel imaging and rapid pulse sequencing, diffusion MRI has been demonstrated as a biomarker of treatment response in breast cancer (31–38), liver cancer (39–47), prostate cancer (34,48), rectal cancer (49–57), lymphomas (20,58–63), head and neck cancer (64,65) and metastases (29,33,37,66–72). Results from clinical studies have shown a significant difference in the mean ADC values between patients responding to treatment relative to patients who were determined to be nonresponsive to treatment.

An example of the clinical application of DW-MRI for the assessment of early treatment response was reported in patients with stage II/III breast cancer treated with neoadjuvant chemotherapy (NAC) (73). Presented in Fig. 2 are representative slices of ADC tumor maps from two patients with breast cancer who underwent two cycles of NAC. The first patient revealed an increase in tumor diffusion values (Fig. 2A), indicating that cell killing had occurred with no significant reduction in tumor size (Fig. 2B). Following the second cycle of treatment, a significant decrease in tumor volume was noted. In the second patient with breast cancer, ADC values remained stable over the treatment period and the patient was subsequently classified as non-pathological complete response (non-pCR) (Fig. 2C, D). These data reveal the tremendous potential of DW-MRI for the early monitoring of cancer treatment response.

Although an initial increase in tumor ADC values during treatment is typically associated with cell death, a subsequent decrease in tumor ADC values may occur, indicating tumor regrowth or, possibly, fibrosis. This present understanding is supported by findings in recurrent high-grade gliomas and osteosarcomas, where lower ADC values are observed in viable tumor and higher ADC values in regions of necrosis following treatment (74,75). Thus, ADC values in the context of the determination of the treatment response should probably be limited to early time intervals post-treatment initiation because of the more complex late-stage cellular processes that may complicate interpretation.

Metastatic lesions pose a very distinct problem for the treatment management of patients with cancer with disseminated disease. In many cases, primary tumors that have metastasized will seed osseous regions. Although bone scans using technetium 99m single photon emission computed tomography (Tc99m-SPECT) imaging are standard clinical practice for the diagnosis of metastatic cancer to the bone, RECIST continues to label bony tumors as 'non-measurable' because of the complex metabolic state of the bone interacting with the tumor. DW-MRI, with its high soft tissue contrast and resolution, has been shown to be highly sensitive to tumor response to therapy, irrespective of bone turnover. In a preliminary pilot study, Lee *et al.* (29) first demonstrated the utility of DW-MRI for therapeutic response assessment in two patients with metastatic prostate cancer to the bone, which was later validated in a large dataset by Reischauer *et al.* (76).

WHOLE-BODY DIFFUSION-WEIGHTED MRI (WBDW-MRI)

Although the aforementioned studies (29,76) focused only on treatment response in individual tumors, advances in wbDW-MRI may allow for multiple lesions to be monitored simultaneously (77,78). This is illustrated in the work by Horger *et al.*

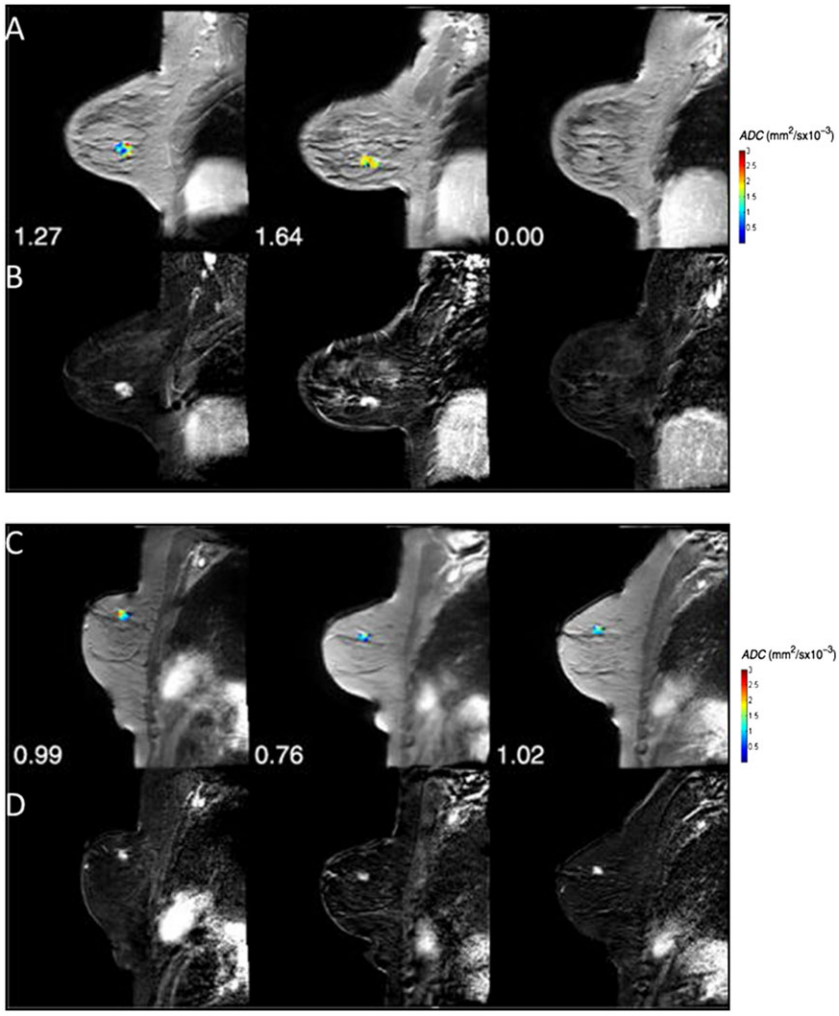

Figure 2. (A) Apparent diffusion coefficient (ADC) maps superimposed on the post-contrast dynamic contrast-enhanced MR (DCE-MR) images at three time points [pre-treatment, after one cycle and after all cycles of neoadjuvant chemotherapy (NAC)] for a patient achieving pathological complete response (pCR). The numbers for each panel represent the mean ADC values for each time point in the parametric map. (B) The difference image between pre-contrast and post-contrast DCE-MRI at each time point. (C) ADC maps superimposed on the post-contrast DCE-MR images at three time points (pre-treatment, after one cycle and after all cycles of NAC) for a non-pCR patient. The numbers for each panel represent the mean ADC values for each time point in the parametric map. (D) The difference image between pre-contrast and post-contrast DCE-MRI at each time point. [Courtesy of and adapted from ref. (73).]

(59), where 20 patients with lymphoma undergoing systemic therapy were monitored using wbDW-MRI. Figure 3 demonstrates the sensitivity of wbDW-MRI for the detection of variations in therapeutic response in a single patient. Multi-focal lesions within the patient were found to have increased ADC values, suggesting that cell killing occurred following treatment, as depicted in these inverted gray-scale images (arrows). In contrast, the large tumor in the pelvic node (arrowhead) revealed a stable ADC value. Through the use of wbDW-MRI, early response assessment can now be obtained over multiple lesions, but at a cost of reduced spatial resolution.

ANOMALIES IN REPORTED DIFFUSION VALUES FOR TUMOR RESPONSE

Most studies have reported that tumor water ADC values typically increase following successful intervention in solid tumors. Although this trend appears to be the norm, there have been cases in which a decrease, rather than an increase, in ADC measurements has been reported to correlate with a positive response (54,79–82). As the tumor mass will respond dynamically throughout the course of fractionated therapies, the timing of the acquired DW-MRI measurement may have an impact on the findings. For example, two studies that investigated the efficacy of DW-MRI on treated rectal cancer (54,80) showed a brief, transient increase in ADC in the first week post-treatment initiation. Subsequently, a decrease in ADC was observed over the next several weeks. Histology confirmed that chemoradiation of rectal carcinoma resulted in increased interstitial fibrosis, which may have had the effect of reducing the ADC values in the tumor regions (54). The authors also drew attention to the fact that regions of obvious necrosis, as observed by MRI within the tumor mass, were not included in the volume of interest prescribed over the tumor mass. Omission of the necrotic regions would bias the measurement to lower ADC values. Therefore, the reported decreased ADC values that correlated with response appear to be primarily related to the timing of the measurement, as well as fibrotic formation following tumor cell death.

NMR IN BIOMEDICINE

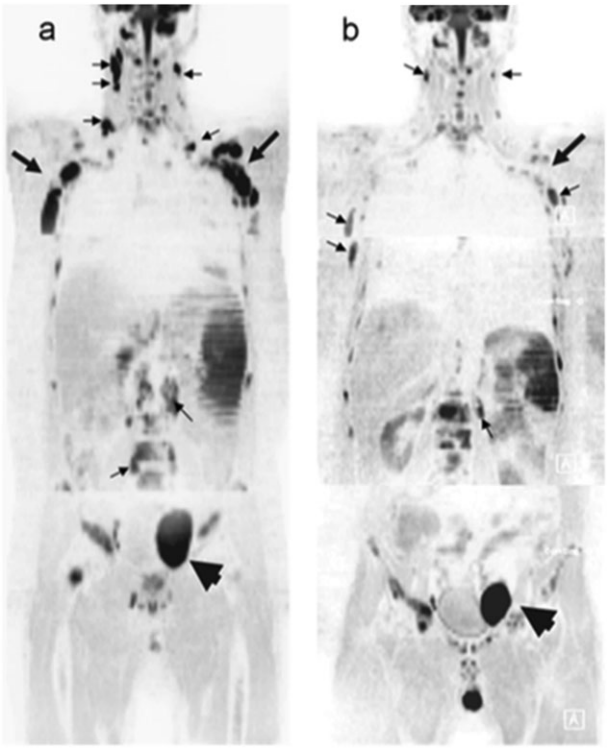

Figure 3. Whole-body diffusion-weighted MRI (wbDW-MRI) is presented as an early indicator of response to systemic therapy in patients with lymphoma. (A) Image of a 48-year-old man diagnosed with diffuse large B-cell lymphoma obtained at baseline shows the ubiquitous involvement of lymph nodes (e.g. cervical and retroperitoneal, small arrows) and axillary regions (large arrows) with marked restriction of water diffusivity. A larger pelvic node (arrowhead) is also seen left of the midline. (B) At day 7 following the institution of chemotherapy with rituximab (anti-CD20 antibodies) + CHOP (cyclophosphamide, hydroxydaunorubicin, vincristine, prednisolone), wbDW-MRI shows evident reduction in signal intensity in the cervical and retroperitoneal node regions (small arrows) and axillary region (large arrows) (from ADC = $0.90/0.33/0.67/0.61 \times 10^{-3}$ mm^2/s to ADC = $1.66/0.73/1.36/1.22 \times 10^{-3}$ mm^2/s), with a corresponding increase in ADC (not shown), but a less marked response, in the pelvic node (arrowhead) (from ADC = $0.83/0.51 \times 10^{-3}$ mm^2/s to ADC = $1.12/0.67 \times 10^{-3}$ mm^2/s) At the interim, the patient achieved complete remission. [Courtesy of ref. (59).]

SPATIAL HETEROGENEITY IN TUMOR RESPONSE

Spatial heterogeneity in tumor response is a major confounding factor in assigning a single indicator to a patient. A given lesion often contains wide gradations of viable cellularity and necrosis, and the response of tumor subregions to treatment can be non-uniform and dependent on many factors. Histogram analysis of ADC values throughout the tumor is one approach to address heterogeneity (83,84). Although a variety of scalar quantities are derivable from tumor ADC histogram analysis, the magnitude of regional changes may be underestimated by whole-tumor summary statistics in the presence of heterogeneous response patterns. Figure 4 from ref. (85) illustrates the effect of response heterogeneity on the tumor histogram. Using simulated data, the authors demonstrated that uniform changes in tumor ADC values result in a mean ADC value that can detect alterations in tumor ADC values (Fig. 4B). Although other whole-tumor metrics may provide more sensitivity, such as the standard deviation for the case in which regions of the tumor demonstrate increasing and decreasing ADC values from baseline (Fig. 4C), we would need to know a priori the most appropriate measure. A more comprehensive evaluation has been performed on the efficacy of histogram-based measures for therapeutic response assessment using MRI-derived blood volume maps in patients with glioma (86). Although not performed using DW-MRI acquired parameters, the study observed negligible effectiveness of a variety of whole-tumor quantitative metrics for the detection of tumor response at both 1 and 3 weeks post-treatment initiation.

An alternative image processing approach has been developed to quantify and spatially map the intrinsic treatment-associated heterogeneity of diffusion values within a tumor. This technique is referred to as 'functional diffusion mapping' (fDM) (87). A key element of fDM is the spatial registration of baseline and follow-up three-dimensional quantitative diffusion maps (i.e. ADC) into a single geometrical space. Further reading on the registration techniques and limitations for therapeutic response assessment is provided in refs. (85,88,89). Once registered, diffusion changes are measured on a voxel-by-voxel basis from spatially aligned pre-treatment and post-treatment initiation ADC maps. Tumor voxels are then classified by their extent of change in ADC. Although fDM was initially evaluated in patients with glioma (87,90–93), this technique has been applied to other tumor types (29,65,76,85). Figure 5 shows fDMs [also referred to as parametric response mapping (PRM_{ADC})] with corresponding scatter plots from patients with head and neck squamous cell carcinoma (HNSCC) diagnosed as complete response (CR) (Fig. 5A) and partial response (PR) (Fig. 5B) following therapy. By analysis of the diffusion maps using fDM, heterogeneity in tumor response can be visualized, with red regions denoting response (i.e. increase in ADC from baseline) *versus* stable and decreased ADC regions depicted as green and blue, respectively. As demonstrated in a variety of tumor types, large regions of increased ADC from baseline (i.e. red voxels) were strongly correlated with treatment response, irrespective of the presence of tumor regions with stable or decreasing ADC values.

STANDARDIZATION AND REPEATABILITY OF ADC MEASUREMENTS

As discussed in this review, the principles and technical feasibility have allowed quantitative DW-MRI to become a clinically viable technique. Nevertheless, for this imaging protocol to become routine in the management of patients and clinical trials, there is a need to standardize DW-MRI acquisition schemes to account for intra and inter-vendor instrument variability (94). In an effort to bring uniformity throughout the various MRI systems, phantoms have been developed to confirm quantitative agreement across platforms. The ideal phantom must be stable throughout the imaging sequences and provide meaningful ADC measurements consistent with biological systems. As a result of the complexity of water diffusion in living tissue, the development of a phantom that is both stable and mimics all tissue properties has its difficulties. Simple fluid-based test objects are the preferred approach to phantom development using fluids that are thermally stable, readily available and safe when properly handled (95,96). In a study by Tofts *et al.* (97), the diffusion coefficients of 15 organic liquids were evaluated and found to stably provide repeatable ADC measurements within the relevant range of biological systems [$(0.36–2.6) \times 10^{-3}$ mm^2/s]. In 2011, Chenevert *et al.* (98) reported a temperature-controlled phantom using water

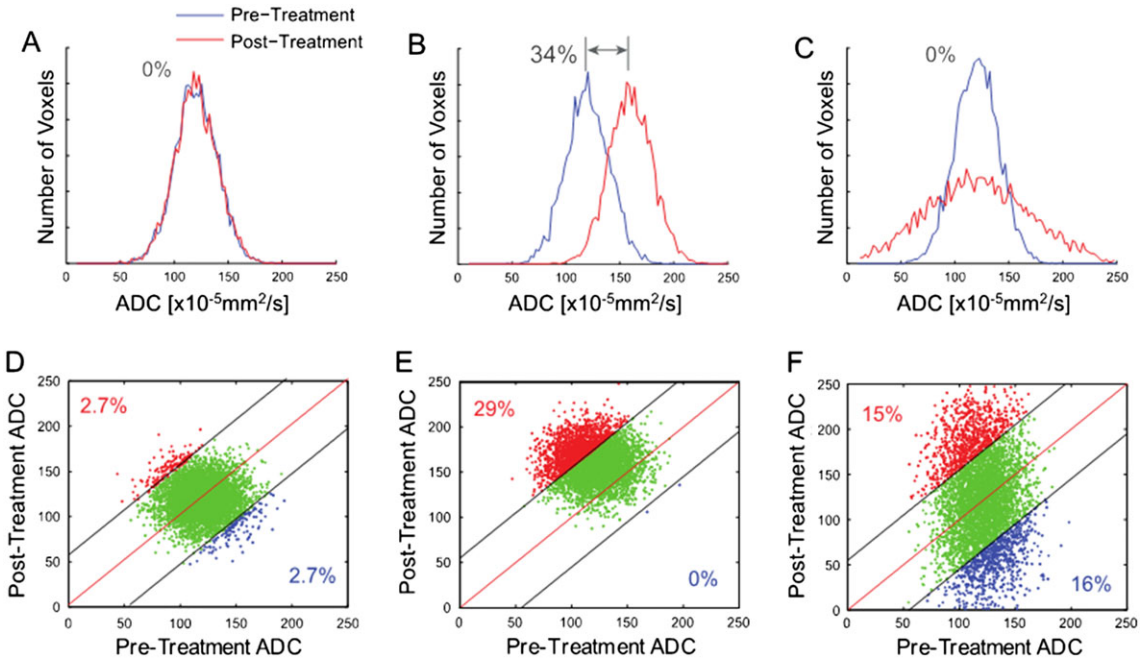

Figure 4. Simulated comparison of whole-tumor histogram analysis (top row; blue line, pre-treatment tumor data; red line, post-treatment tumor data) *versus* the corresponding voxel-based analysis using a joint density histogram (bottom row). Histograms from tumors with no major change (A), significant uniform shift to higher apparent diffusion coefficient (ADC) values with a 34% net mean change (B) and heterogeneous ADC changes (increased and decreased ADC values) resulting in no net detectable histogram shift (C). Parametric response maps from the corresponding histograms are also shown, where, in (D), the confidence interval for the detection of change was set to 95%, and thus no significant change in red voxels (increased values) or blue voxels (decreased values) was detected. (E) An increase in the number of red voxels was detected at 29% of the total tumor voxels. (F) Both an increase and a decrease in tumor voxels of approximately 15% were detected, whereas no major shift was detected using a histogram analysis of the same data (C). [Courtesy of Ref. (85).]

cooled to near freezing. This phantom consisted of liquid water jacketed with ice water, such that the inner chamber was cooled to ~0 °C. Although water diffusivity is highly sensitive to temperature (99), jacketing the liquid water with ice allowed a stable environment with temperatures maintained for up to 4 h and a reliable, biologically relevant ADC value (~1 × 10^{-3} mm^2/s). The availability of stable and reproducible phantoms has allowed multi-center studies to be performed, demonstrating the repeatability of quantitative DW-MRI across platforms (100,101).

In the absence of a standard DW-MRI protocol, investigators of clinical trials are employing strategies to contend with intra-instrument variability. Affectionately referred to as the 'coffee-break exam', this approach acquires repeat DW-MRI examinations, minutes to hours apart, to ascertain the variability in the ADC measurement prior to therapeutic intervention. The motivation of this strategy is to characterize the noise associated with the ADC measurement for a given patient and platform in the absence of disease- or treatment-related changes in tumor physiology and anatomy. Various studies, just to name a few, have reported stable quantitative DW-MRI measurements in HNSCCs (64), hepatocellular carcinoma (102), malignant lung lesions (103), rectal cancer (104) and primary breast cancer (105). Until uniformity in DW-MRI protocols between vendors, instruments and sites is obtained, the strategy of repeat examinations prior to therapeutic intervention will help to alleviate some of the variability in the ADC measurement within a given instrument.

FUTURE DIRECTIONS

The studies presented here support the use of DW-MRI as an early surrogate biomarker for tumor response assessment. In a growing body of literature, changes in tumor water diffusion values have been reported to correlate with response to therapy, despite the diverse set of tumor types, MRI manufacturers and magnetic field strengths used to collect the data, together with the varying approaches used to analyse the datasets (Figure 6, Table 1). Taken together, this reveals the overall robustness of DW-MRI for oncological treatment assessment. Clinical cancer studies on the efficacy of DW-MRI as a surrogate imaging biomarker of the tumor treatment response have demonstrated that treatment-induced cell death can be detected in responding tumors as an increased ADC value in these regions. As a result of variability in DW-MRI acquisition and analytical post-processing protocols, efforts have solidified in the publication of a consensus paper to provide for standardization across institutions (16). In addition, temperature-controlled phantoms have recently been developed to facilitate multi-center DW-MRI clinical trials (100,101). These standards are needed for data acquisition, post-image processing, timing of evaluation and the method used to generate the quantifiable metric used to report treatment response. Although the momentum for the use of DW-MRI in the context of tumor response assessment is continuing to grow, validation of DW-MRI as a surrogate imaging biomarker of response will require a large, prospective, multi-institutional trial performed in a standardized fashion between sites. Analysis of the data could also be useful for the validation of the image post-processing software and for regulatory approval as a device. Having a Food and Drug Administration (FDA)- or European-approved software package would provide additional momentum for enhancing the probability that DW-MRI will ultimately be incorporated into routine clinical practice for the management of patients with cancer.

NMR IN BIOMEDICINE

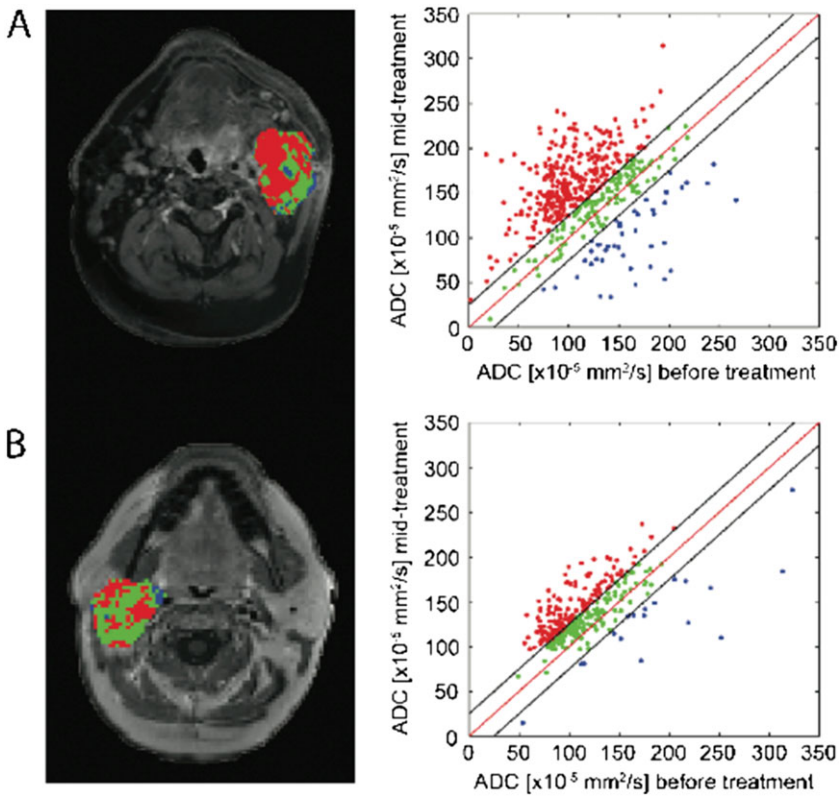

Figure 5. Functional diffusion mapping (fDM) applied to clinical data acquired from patients with head and neck squamous cell carcinoma (HNSCC) diagnosed as pCR (pathological complete response) (A) and PR (partial response) (B). Results from the fDM analysis are presented as color-coded maps superimposed on contrast-enhanced T_1-weighted images and scatter plots with axes pre-treatment ADC (*x*-axis) and post-treatment ADC (*y*-axis). Color-coding is as follows: red, increased ADC values; blue, decreased ADC values; green, unchanged ADC values. [Courtesy of ref. (65).]

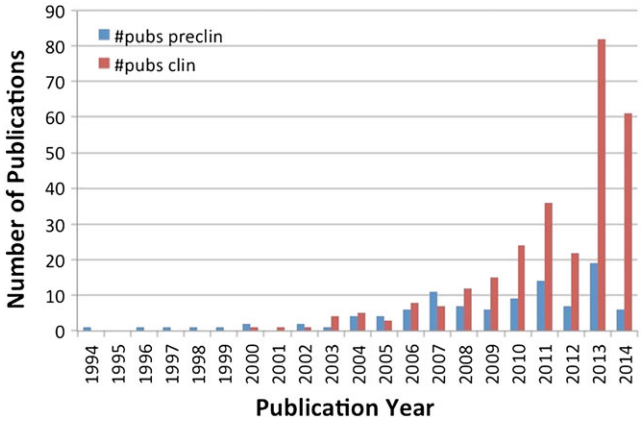

Figure 6. Number of annual publications on the application of diffusion-weighted MRI (DW-MRI) for therapeutic response assessment. Yearly evaluation showed a growing increase in the number of studies demonstrating the efficacy of DW-MRI for cancer response to treatment. The search was performed on Pubmed using the following criteria [((diffusion OR ADC OR "apparent diffusion coefficient") AND MRI AND response) NOT (stroke OR review)]. Individual references were manually evaluated.

Table 1. Studies of Therapeutic Response by DW-MRI

Site	Reference
Abdominal	(109)
Acoustic neuroma	(110)
Bladder	(111,112)
Bone marrow	(113)
Brain	(26,87,93,114–138)
Breast	(35–38,139–152)
Cervical	(153–160)
Eye	(161,162)
Leiomyoma	(163–165)
Liver	(41,42,44,46,70,166–181)
Lung	(182–185)
Lymphoma	(186–188)
Myeloma	(189,190)
Ovarian	(191–193)
Pancreas	(194)
Prostate	(29,195–198)
Rectal	(54,79,199–207)
Sarcoma	(208–214)
HNSCC	(65,215–220)

[1]HNSCC, head and neck squamous cell carcinoma.

Future opportunities in employing DW-MRI in the clinical management of patients with cancer may include adaptive therapy protocols based on intra-therapy evaluation of early ADC changes during fractionated dosage schedules, allowing for the modification of interventions and for the quantification of multi-focal disease response using wbDW-MRI (78). Finally, the recent emergence of anticancer immunotherapies raises an urgent need for the establishment of radiological metrics for

assessment of the response to such experimental interventions (106–108). Further efforts investigating advanced imaging techniques, such as DW-MRI, are needed to delineate its ability to provide meaningful insights into treatment responsiveness in order for it to have a successful impact on clinical decision making.

Acknowledgements

Funding support for this work was provided by the National Institutes of Health grants P01CA085878, U01CA166104 and R35CA197701.

REFERENCES

1. Gehan EA, Schneiderman MA. Historical and methodological developments in clinical trials at the National Cancer Institute. Stat. Med. 1990; 9(8): 871–80 discussion 903–906.
2. Eisenhauer EA, Therasse P, Bogaerts J, Schwartz LH, Sargent D, Ford R, Dancey J, Arbuck S, Gwyther S, Mooney M, Rubinstein L, Shankar L, Dodd L, Kaplan R, Lacombe D, Verweij J. New response evaluation criteria in solid tumours: revised RECIST guideline (version 1.1). Eur. J. Cancer 2009; 45(2): 228–247.
3. Wen PY, Macdonald DR, Reardon DA, Cloughesy TF, Sorensen AG, Galanis E, Degroot J, Wick W, Gilbert MR, Lassman AB, Tsien C, Mikkelsen T, Wong ET, Chamberlain MC, Stupp R, Lamborn KR, Vogelbaum MA, van den Bent MJ, Chang SM. Updated response assessment criteria for high-grade gliomas: response assessment in neuro-oncology working group. J. Clin. Oncol. 2010; 28(11): 1963–1972.
4. World Health Organization (WHO). *WHO Handbook for Reporting Results of Cancer Treatment*. Geneva: WHO; 1979.
5. Jaffe CC. Measures of response: RECIST, WHO, and new alternatives. J. Clin. Oncol. 2006; 24(20): 3245–3251.
6. Choi H, Charnsangavej C, de Castro Faria S, Tamm EP, Benjamin RS, Johnson MM, Macapinlac HA, Podoloff DA. CT evaluation of the response of gastrointestinal stromal tumors after imatinib mesylate treatment: a quantitative analysis correlated with FDG PET findings. Am. J. Roentgenol. 2004; 183(6): 1619–1628.
7. Strumberg D, Richly H, Hilger RA, Schleucher N, Korfee S, Tewes M, Faghih M, Brendel E, Voliotis D, Haase CG, Schwartz B, Awada A, Voigtmann R, Scheulen ME, Seeber S. Phase I clinical and pharmacokinetic study of the novel Raf kinase and vascular endothelial growth factor receptor inhibitor BAY 43-9006 in patients with advanced refractory solid tumors. J. Clin. Oncol. 2005; 23(5): 965–972.
8. Barrington SF, Mikhaeel NG, Kostakoglu L, Meignan M, Hutchings M, Mueller SP, Schwartz LH, Zucca E, Fisher RI, Trotman J, Hoekstra OS, Hicks RJ, O'Doherty MJ, Hustinx R, Biggi A, Cheson BD. Role of imaging in the staging and response assessment of lymphoma: consensus of the International Conference on Malignant Lymphomas Imaging Working Group. J. Clin. Oncol. 2014; 32(27): 3048–3058.
9. Cheson BD, Fisher RI, Barrington SF, Cavalli F, Schwartz LH, Zucca E, Lister TA, Alliance AL, Lymphoma G, Eastern Cooperative Oncology G, European Mantle Cell Lymphoma C, Italian Lymphoma F, European Organisation for R, Treatment of Cancer/Dutch Hemato-Oncology G, Grupo Espanol de Medula O, German High-Grade Lymphoma Study G, German Hodgkin's Study G, Japanese Lymphorra Study G, Lymphoma Study A, Group NCT, Nordic Lymphoma Study G, Southwest Oncology G, United Kingdom National Cancer Research I. Recommendations for initial evaluation, staging, and response assessment of Hodgkin and non-Hodgkin lymphoma: the Lugano classification. J. Clin. Oncol. 2014; 32(27): 3059–3068.
10. Stejskal E, Tanner J. Spin diffusion measurements: spin echoes in the presence of a time-dependent field gradient. J. Chem. Phys. 1965; 42(1): 288–292.
11. Thomsen C, Henriksen O, Ring P. In vivo measurement of water self diffusion in the human brain by magnetic resonance imaging. Acta Radiol. 1987; 28(3): 353–361.
12. Merboldt KD, Bruhn H, Frahm J, Gyngell ML, Hanicke W, Deimling M. MRI of "diffusion" in the human brain: new results using a modified CE-FAST sequence. Magn. Reson. Med. 1989; 9(3): 423–429.
13. Le Bihan D, Breton E, Lallemand D, Aubin ML, Vignaud J, Laval-Jeantet M. Separation of diffusion and perfusion in intravoxel incoherent motion MR imaging. Radiology 1988; 168(2): 497–505.
14. Le Bihan D. Molecular diffusion nuclear magnetic resonance imaging. Magn. Reson. Q. 1991; 7(1): 1–30.
15. Bammer R. Basic principles of diffusion-weighted imaging. Eur. J. Radiol. 2003; 45(3): 169–184.
16. Padhani AR, Liu G, Koh DM, Chenevert TL, Thoeny HC, Takahara T, Dzik-Jurasz A, Ross BD, Van Cauteren M, Collins D, Hammoud DA, Rustin GJ, Taouli B, Choyke PL. Diffusion-weighted magnetic resonance imaging as a cancer biomarker: consensus and recommendations. Neoplasia 2009; 11(2): 102–125.
17. Edelman RR, Wielopolski P, Schmitt F. Echo-planar MR imaging. Radiology 1994; 192(3): 600–612.
18. Hamstra DA, Rehemtulla A, Ross BD. Diffusion magnetic resonance imaging: a biomarker for treatment response in oncology. J. Clin. Oncol. 2007; 25(26): 4104–4109.
19. Lyng H, Haraldseth O, Rofstad EK. Measurement of cell density and necrotic fraction in human melanoma xenografts by diffusion weighted magnetic resonance imaging. Magn. Reson. Med. 2000; 43(6): 828–836.
20. Guo AC, Cummings TJ, Dash RC, Provenzale JM. Lymphomas and high-grade astrocytomas: comparison of water diffusibility and histologic characteristics. Radiology 2002; 224(1): 177–183.
21. Chenevert TL, Stegman LD, Taylor JM, Robertson PL, Greenberg HS, Rehemtulla A, Ross BD. Diffusion magnetic resonance imaging: an early surrogate marker of therapeutic efficacy in brain tumors. J. Natl. Cancer Inst. 2000; 92(24): 2029–2036.
22. Chenevert TL, McKeever PE, Ross BD. Monitoring early response of experimental brain tumors to therapy using diffusion magnetic resonance imaging. Clin. Cancer Res. 1997; 3(9): 1457–1466.
23. Le Bihan D. The 'wet mind': water and functional neuroimaging. Phys. Med. Biol. 2007; 52(7): R57–90.
24. Chenevert TL, Sundgren PC, Ross BD. Diffusion imaging: insight to cell status and cytoarchitecture. Neuroimaging Clin. N. Am. 2006; 16(4): 619–632 viii–ix.
25. Ross BD, Moffat BA, Lawrence TS, Mukherji SK, Gebarski SS, Quint DJ, Johnson TD, Junck L, Robertson PL, Muraszko KM, Dong Q, Meyer CR, Bland PH, McConville P, Geng H, Rehemtulla A, Chenevert TL. Evaluation of cancer therapy using diffusion magnetic resonance imaging. Mol. Cancer Ther. 2003; 2(6): 581–587.
26. Huang CF, Chou HH, Tu HT, Yang MS, Lee JK, Lin LY. Diffusion magnetic resonance imaging as an evaluation of the response of brain metastases treated by stereotactic radiosurgery. Surg. Neurol. 2008; 69(1): 62–68 discussion 68.
27. Lee KC, Hamstra DA, Bhojani MS, Khan AP, Ross BD, Rehemtulla A. Noninvasive molecular imaging sheds light on the synergy between 5-fluorouracil and TRAIL/Apo2L for cancer therapy. Clin. Cancer Res. 2007; 13(6): 1839–1846.
28. Lee KC, Hall DE, Hoff BA, Moffat BA, Sharma S, Chenevert TL, Meyer CR, Leopold WR, Johnson TD, Mazurchuk RV, Rehemtulla A, Ross BD. Dynamic imaging of emerging resistance during cancer therapy. Cancer Res. 2006; 66(9): 4687–4892.
29. Lee KC, Bradley DA, Hussain M, Meyer CR, Chenevert TL, Jacobson JA, Johnson TD, Galban CJ, Rehemtulla A, Pienta KJ, Ross BD. A feasibility study evaluating the functional diffusion map as a predictive imaging biomarker for detection of treatment response in a patient with metastatic prostate cancer to the bone. Neoplasia 2007; 9(12): 1003–1011.
30. Hamstra DA, Lee KC, Tychewicz JM, Schepkin VD, Moffat BA, Chen M, Dornfeld KJ, Lawrence TS, Chenevert TL, Ross BD, Gelovani JT, Rehemtulla A. The use of ^{19}F spectroscopy and diffusion-weighted MRI to evaluate differences in gene-dependent enzyme prodrug therapies. Mol. Ther. 2004; 10(5): 916–928.
31. Bufi E, Belli P, Di Matteo M, Terribile D, Franceschini G, Nardone L, Petrone G, Bonomo L. Effect of breast cancer phenotype on diagnostic performance of MRI in the prediction to response to neoadjuvant treatment. Eur. J. Radiol. 2014; 83(9): 1631–1638.
32. Chinnaiyan AM, Prasad U, Shankar S, Hamstra DA, Shanaiah M, Chenevert TL, Ross BD, Rehemtulla A. Combined effect of tumor necrosis factor-related apoptosis-inducing ligand and ionizing radiation in breast cancer therapy. Proc. Natl. Acad. Sci. USA 2000; 97(4): 1754–1759.
33. Gaeta M, Benedetto C, Minutoli F, D'Angelo T, Amato E, Mazziotti S, Racchiusa S, Mormina E, Blandino A, Pergolizzi S. Use of diffusion-weighted, intravoxel incoherent motion, and dynamic

contrast-enhanced MR imaging in the assessment of response to radiotherapy of lytic bone metastases from breast cancer. Acad. Radiol. 2014; 21(10): 1286–1293.
34. Liu L, Wu N, Ouyang H, Dai JR, Wang WH. Diffusion-weighted MRI in early assessment of tumour response to radiotherapy in high-risk prostate cancer. Br. J. Radiol. 2014; 87(1043): 20140359.
35. Pickles MD, Gibbs P, Lowry M, Turnbull LW. Diffusion changes precede size reduction in neoadjuvant treatment of breast cancer. Magn. Reson. Imaging 2006; 24(7): 843–847.
36. Sharma U, Danishad KK, Seenu V, Jagannathan NR. Longitudinal study of the assessment by MRI and diffusion-weighted imaging of tumor response in patients with locally advanced breast cancer undergoing neoadjuvant chemotherapy. NMR Biomed. 2009; 22(1): 104–113.
37. Theilmann RJ, Borders R, Trouard TP, Xia G, Outwater E, Ranger-Moore J, Gillies RJ, Stopeck A. Changes in water mobility measured by diffusion MRI predict response of metastatic breast cancer to chemotherapy. Neoplasia 2004; 6(6): 831–837.
38. Yankeelov TE, Lepage M, Chakravarthy A, Broome EE, Niermann KJ, Kelley MC, Meszoely I, Mayer IA, Herman CR, McManus K, Price RR, Gore JC. Integration of quantitative DCE-MRI and ADC mapping to monitor treatment response in human breast cancer: initial results. Magn. Reson. Imaging 2007; 25(1): 1–13.
39. Bonekamp S, Jolepalem P, Lazo M, Gulsun MA, Kiraly AP, Kamel IR. Hepatocellular carcinoma: response to TACE assessed with semiautomated volumetric and functional analysis of diffusion-weighted and contrast-enhanced MR imaging data. Radiology 2011; 260(3): 752–761.
40. Corona-Villalobos CP, Halappa VG, Geschwind JF, Bonekamp S, Reyes D, Cosgrove D, Pawlik TM, Kamel IR. Volumetric assessment of tumour response using functional MR imaging in patients with hepatocellular carcinoma treated with a combination of doxorubicin-eluting beads and sorafenib. Eur. Radiol. 2014; 25: 380–390.
41. Deng J, Miller FH, Rhee TK, Sato KT, Mulcahy MF, Kulik LM, Salem R, Omary RA, Larson AC. Diffusion-weighted MR imaging for determination of hepatocellular carcinoma response to yttrium-90 radioembolization. J. Vasc. Interv. Radiol. 2006; 17(7): 1195–2200.
42. Kamel IR, Bluemke DA, Eng J, Liapi E, Messersmith W, Reyes DK, Geschwind JF. The role of functional MR imaging in the assessment of tumor response after chemoembolization in patients with hepatocellular carcinoma. J. Vasc. Intervent. Radiol. 2006; 17(3): 505–512.
43. Kamel IR, Liapi E, Reyes DK, Zahurak M, Bluemke DA, Geschwind JF. Unresectable hepatocellular carcinoma: serial early vascular and cellular changes after transarterial chemoembolization as detected with MR imaging. Radiology 2009; 250(2): 466–473.
44. Kamel IR, Reyes DK, Liapi E, Bluemke DA, Geschwind JF. Functional MR imaging assessment of tumor response after ^{90}Y microsphere treatment in patients with unresectable hepatocellular carcinoma. J. Vasc. Intervent. Radiol. 2007; 18(1 Pt 1): 49–56.
45. Mannelli L, Kim S, Hajdu CH, Babb JS, Taouli B. Serial diffusion-weighted MRI in patients with hepatocellular carcinoma: prediction and assessment of response to transarterial chemoembolization. Preliminary experience. Eur. J. Radiol. 2013; 82(4): 577–582.
46. Rhee TK, Naik NK, Deng J, Atassi B, Mulcahy MF, Kulik LM, Ryu RK, Miller FH, Larson AC, Salem R, Omary RA. Tumor response after yttrium-90 radioembolization for hepatocellular carcinoma: comparison of diffusion-weighted functional MR imaging with anatomic MR imaging. J. Vasc. Intervent. Radiol. 2008; 19(8): 1180–1186.
47. Yu JS, Kim JH, Chung JJ, Kim KW. Added value of diffusion-weighted imaging in the MRI assessment of perilesional tumor recurrence after chemoembolization of hepatocellular carcinomas. J. Magn. Reson. Imaging 2009; 30(1): 153–160.
48. Zelhof B, Pickles M, Liney G, Gibbs P, Rodrigues G, Kraus S, Turnbull L. Correlation of diffusion-weighted magnetic resonance data with cellularity in prostate cancer. BJU Int. 2009; 103: 883–888.
49. Barbaro B, Vitale R, Valentini V, Illuminati S, Vecchio FM, Rizzo G, Gambacorta MA, Coco C, Crucitti A, Persiani R, Sofo L, Bonomo L. Diffusion-weighted magnetic resonance imaging in monitoring rectal cancer response to neoadjuvant chemoradiotherapy. Int. J. Radiat. Oncol. Biol. Phys. 2012; 83(2): 594–599.
50. Birlik B, Obuz F, Elibol FD, Celik AO, Sokmen S, Terzi C, Sagol O, Sarioglu S, Gorken I, Oztop L. Diffusion-weighted MRI and MR-volumetry in the evaluation of tumor response after preoperative chemoradiotherapy in patients with locally advanced rectal cancer. Magn. Reson. Imaging 2015; 33: 201–212.
51. Carbone SF, Pirtoli L, Ricci V, Carfagno T, Tini P, Lazzi S, Volterrani L. Diffusion-weighted MR volumetry for assessing the response of rectal cancer to combined radiation therapy with chemotherapy. Radiology 2012; 263(1): 311.
52. Carbone SF, Pirtoli L, Ricci V, Venezia D, Carfagno T, Lazzi S, Mourmouras V, Lorenzi B, Volterrani L. Assessment of response to chemoradiation therapy in rectal cancer using MR volumetry based on diffusion-weighted data sets: a preliminary report. Radiol. Med. 2012; 117(7): 1112–1124.
53. Genovesi D, Filippone A, Ausili Cefaro G, Trignani M, Vinciguerra A, Augurio A, Di Tommaso M, Borzillo V, Sabatino F, Innocenti P, Liberatore E, Colecchia G, Tartaro A, Cotroneo AR. Diffusion-weighted magnetic resonance for prediction of response after neoadjuvant chemoradiation therapy for locally advanced rectal cancer: preliminary results of a monoinstitutional prospective study. Eur. J. Surg. Oncol. 2013; 39(10): 1071–1078.
54. Hein PA, Kremser C, Judmaier W, Griebel J, Pfeiffer KP, Kreczy A, Hug EB, Lukas P, DeVries AF. Diffusion-weighted magnetic resonance imaging for monitoring diffusion changes in rectal carcinoma during combined, preoperative chemoradiation: preliminary results of a prospective study. Eur. J. Radiol. 2003; 45(3): 214–222.
55. Ippolito D, Monguzzi L, Guerra L, Deponti E, Gardani G, Messa C, Sironi S. Response to neoadjuvant therapy in locally advanced rectal cancer: assessment with diffusion-weighted MR imaging and ^{18}FDG PET/CT. Abdom. Imaging 2012; 37(6): 1032–1040.
56. Kim SH, Lee JM, Hong SH, Kim GH, Lee JY, Han JK, Choi BI. Locally advanced rectal cancer: added value of diffusion-weighted MR imaging in the evaluation of tumor response to neoadjuvant chemo- and radiation therapy. Radiology 2009; 253(1): 116–125.
57. Kim SH, Ryu KH, Yoon JH, Lee Y, Paik JH, Kim SJ, Jung HK, Lee KH. Apparent diffusion coefficient for lymph node characterization after chemoradiation therapy for locally advanced rectal cancer. Acta Radiol. 2015; 56: 1446–1453.
58. De Paepe K, Bevernage C, De Keyzer F, Wolter P, Gheysens O, Janssens A, Oyen R, Verhoef G, Vandecaveye V. Whole-body diffusion-weighted magnetic resonance imaging at 3 Tesla for early assessment of treatment response in non-Hodgkin lymphoma: a pilot study. Cancer Imaging 2013; 13: 53–62.
59. Horger M, Claussen C, Kramer U, Fenchel M, Lichy M, Kaufmann S. Very early indicators of response to systemic therapy in lymphoma patients based on alterations in water diffusivity—a preliminary experience in 20 patients undergoing whole-body diffusion-weighted imaging. Eur. J. Radiol. 2014; 83(9): 1655–1664.
60. Montoro J, Laszlo D, Zing NP, Petralia G, Conte G, Colandrea M, Martinelli G, Preda L. Comparison of whole-body diffusion-weighted magnetic resonance and FDG-PET/CT in the assessment of Hodgkin's lymphoma for staging and treatment response. Ecancermedicalscience 2014; 8: 429.
61. Prat MC, Surapaneni K, Chalian H, DeLaPaz RL, Kazim M. Ocular adnexal lymphoma: monitoring response to therapy with diffusion-weighted imaging. Ophth. Plast. Reconstruct. Surg. 2013; 29(6): 424–427.
62. Siegel MJ, Jokerst CE, Rajderkar D, Hildebolt CF, Goyal S, Dehdashti F, Wagner Johnston N, Siegel BA. Diffusion-weighted MRI for staging and evaluation of response in diffuse large B-cell lymphoma: a pilot study. NMR Biomed. 2014; 27(6): 681–691.
63. Tsuji K, Kishi S, Tsuchida T, Yamauchi T, Ikegaya S, Urasaki Y, Fujiwara Y, Ueda T, Okazawa H, Kimura H. Evaluation of staging and early response to chemotherapy with whole-body diffusion-weighted MRI in malignant lymphoma patients: a comparison with FDG-PET/CT. J. Magn. Reson. Imaging 2015; 41: 1601–1607.
64. Ding Y, Fuller C, Mohamed A, Wang J, Hazle J. TU-F-CAMPUS-I-01: head and neck squamous cell carcinoma: short-term repeatability of apparent diffusion coefficient and intravoxel incoherent motion parameters at 3.0T. Med. Phys. 2015; 42(6): 3646.
65. Galban CJ, Mukherji SK, Chenevert TL, Meyer CR, Hamstra DA, Bland PH, Johnson TD, Moffat BA, Rehemtulla A, Eisbruch A, Ross BD. A feasibility study of parametric response map analysis of diffusion-weighted magnetic resonance imaging scans of head and neck cancer patients for providing early detection of therapeutic efficacy. Transl. Oncol. 2009; 2(3): 184–190.

66. Blackledge MD, Collins DJ, Tunariu N, Orton MR, Padhani AR, Leach MO, Koh DM. Assessment of treatment response by total tumor volume and global apparent diffusion coefficient using diffusion-weighted MRI in patients with metastatic bone disease: a feasibility study. PloS One 2014; 9(4): e91779.
67. Byun WM, Shin SO, Chang Y, Lee SJ, Finsterbusch J, Frahm J. Diffusion-weighted MR imaging of metastatic disease of the spine: assessment of response to therapy. Am. J. Neuroradiol. 2002; 23(6): 906–9\12.
68. Cui Y, Zhang XP, Sun YS, Tang L, Shen L. Apparent diffusion coefficient: potential imaging biomarker for prediction and early detection of response to chemotherapy in hepatic metastases. Radiology 2008; 248(3): 894–900.
69. Kukuk GM, Murtz P, Traber F, Meyer C, Ullrich J, Gieseke J, Ahmadzadehfar H, Ezziddin S, Schild HH, Willinek WA. Diffusion-weighted imaging with acquisition of three b-values for response evaluation of neuroendocrine liver metastases undergoing selective internal radiotherapy. Eur. Radiol. 2014; 24(2): 267–276.
70. Marugami N, Tanaka T, Kitano S, Hirohashi S, Nishiofuku H, Takahashi A, Sakaguchi H, Matsuoka M, Otsuji T, Takahama J, Higashiura W, Kichikawa K. Early detection of therapeutic response to hepatic arterial infusion chemotherapy of liver metastases from colorectal cancer using diffusion-weighted MR imaging. Cardiovasc. Intervent. Radiol. 2009; 32(4): 638–646.
71. Mungai F, Pasquinelli F, Mazzoni LN, Virgili G, Ragozzino A, Quaia E, Morana G, Giovagnoni A, Grazioli L, Colagrande S. Diffusion-weighted magnetic resonance imaging in the prediction and assessment of chemotherapy outcome in liver metastases. Radiol. Med. 2014; 119(8): 625–633.
72. Schmidt S, Dunet V, Koehli M, Montemurro M, Meuli R, Prior JO. Diffusion-weighted magnetic resonance imaging in metastatic gastrointestinal stromal tumor (GIST): a pilot study on the assessment of treatment response in comparison with ^{18}F-FDG PET/CT. Acta Radiol. 2013; 54(8): 837–842.
73. Li X, Abramson RG, Arlinghaus LR, Kang H, Chakravarthy AB, Abramson VG, Farley J, Mayer IA, Kelley MC, Meszoely IM, Means-Powell J, Grau AM, Sanders M, Yankeelov TE. Multiparametric magnetic resonance imaging for predicting pathological response after the first cycle of neoadjuvant chemotherapy in breast cancer. Invest. Radiol. 2015; 50: 195–204.
74. Uhl M, Saueressig U, van Buiren M, Kontny U, Niemeyer C, Kohler G, Ilyasov K, Langer M. Osteosarcoma: preliminary results of in vivo assessment of tumor necrosis after chemotherapy with diffusion- and perfusion-weighted magnetic resonance imaging. Invest. Radiol. 2006; 41(8): 618–623.
75. Hein PA, Eskey CJ, Dunn JF, Hug EB. Diffusion-weighted imaging in the follow-up of treated high-grade gliomas: tumor recurrence versus radiation injury. Am. J. Neuroradiol. 2004; 25(2): 201–209.
76. Reischauer C, Froehlich JM, Koh DM, Graf N, Padevit C, John H, Binkert CA, Boesiger P, Gutzeit A. Bone metastases from prostate cancer: assessing treatment response by using diffusion-weighted imaging and functional diffusion maps—initial observations. Radiology 2010; 257(2): 523–531.
77. Takahara T, Imai Y, Yamashita T, Yasuda S, Nasu S, Van Cauteren M. Diffusion weighted whole body imaging with background body signal suppression (DWIBS): technical improvement using free breathing, STIR and high resolution 3D display. Radiat. Med. 2004; 22(4): 275–282.
78. Kwee TC, Takahara T, Ochiai R, Nievelstein RA, Luijten PR. Diffusion-weighted whole-body imaging with background body signal suppression (DWIBS): features and potential applications in oncology. Eur. Radiol. 2008; 18(9): 1937–1952.
79. Dzik-Jurasz A, Domenig C, George M, Wolber J, Padhani A, Brown G, Doran S. Diffusion MRI for prediction of response of rectal cancer to chemoradiation. Lancet 2002; 360(9329): 307–308.
80. Kremser C, Judmaier W, Hein P, Griebel J, Lukas P, de Vries A. Preliminary results on the influence of chemoradiation on apparent diffusion coefficients of primary rectal carcinoma measured by magnetic resonance imaging. Strahlenther. Onkol. 2003; 179(9): 641–649.
81. Jacobs MA, Herskovits EH, Kim HS. Uterine fibroids: diffusion-weighted MR imaging for monitoring therapy with focused ultrasound surgery—preliminary study. Radiology 2005; 236(1): 196–203.
82. Aliu SO, Wilmes LJ, Moasser MM, Hann BC, Li KL, Wang D, Hylton NM. MRI methods for evaluating the effects of tyrosine kinase inhibitor administration used to enhance chemotherapy efficiency in a breast tumor xenograft model. J. Magn. Reson. Imaging 2009; 29(5): 1071–1079.
83. Just N. Improving tumour heterogeneity MRI assessment with histograms. Br. J. Cancer 2014; 111(12): 2205–2213.
84. Woo S, Cho JY, Kim SY, Kim SH. Histogram analysis of apparent diffusion coefficient map of diffusion-weighted MRI in endometrial cancer: a preliminary correlation study with histological grade. Acta Radiol. 2014; 55(10): 1270–1277.
85. Boes JL, Hoff BA, Hylton N, Pickles MD, Turnbull LW, Schott AF, Rehemtulla A, Chamberlain R, Lemasson B, Chenevert TL, Galb NC, Meyer CR, Ross BD. Image registration for quantitative parametric response mapping of cancer treatment response. Transl. Oncol. 2014; 7(1): 101–110.
86. Lemasson B, Chenevert TL, Lawrence TS, Tsien C, Sundgren PC, Meyer CR, Junck L, Boes J, Galban S, Johnson TD, Rehemtulla A, Ross BD, Galban CJ. Impact of perfusion map analysis on early survival prediction accuracy in glioma patients. Transl. Oncol. 2013; 6(6): 766–774.
87. Moffat BA, Chenevert TL, Lawrence TS, Meyer CR, Johnson TD, Dong Q, Tsien C, Mukherji S, Quint DJ, Gebarski SS, Robertson PL, Junck LR, Rehemtulla A, Ross BD. Functional diffusion map: a noninvasive MRI biomarker for early stratification of clinical brain tumor response. Proc. Natl. Acad. Sci. USA 2005; 102(15): 5524–5529.
88. Li X, Dawant BM, Welch EB, Chakravarthy AB, Freehardt D, Mayer I, Kelley M, Meszoely I, Gore JC, Yankeelov TE. A nonrigid registration algorithm for longitudinal breast MR images and the analysis of breast tumor response. Magn. Reson. Imaging 2009; 27(9): 1258–1270.
89. Li X, Dawant BM, Welch EB, Chakravarthy AB, Xu L, Mayer I, Kelley M, Meszoely I, Means-Powell J, Gore JC, Yankeelov TE. Validation of an algorithm for the nonrigid registration of longitudinal breast MR images using realistic phantoms. Med. Phys. 2010; 37(6): 2541–1552.
90. Ellingson BM, Cloughesy TF, Lai A, Nghiemphu PL, Liau LM, Pope WB. Quantitative probabilistic functional diffusion mapping in newly diagnosed glioblastoma treated with radiochemotherapy. Neuro-oncology 2013; 15(3): 382–390.
91. Ellingson BM, Cloughesy TF, Zaw T, Lai A, Nghiemphu PL, Harris R, Lalezari S, Wagle N, Naeini KM, Carrillo J, Liau LM, Pope WB. Functional diffusion maps (fDMs) evaluated before and after radiochemotherapy predict progression-free and overall survival in newly diagnosed glioblastoma. Neuro-oncology 2012; 14(3): 333–343.
92. Hamstra DA, Chenevert TL, Moffat BA, Johnson TD, Meyer CR, Mukherji SK, Quint DJ, Gebarski SS, Fan X, Tsien CI, Lawrence TS, Junck L, Rehemtulla A, Ross BD. Evaluation of the functional diffusion map as an early biomarker of time-to-progression and overall survival in high-grade glioma. Proc. Natl. Acad. Sci. USA 2005; 102(46): 16 759–764.
93. Hamstra DA, Galban CJ, Meyer CR, Johnson TD, Sundgren PC, Tsien C, Lawrence TS, Junck L, Ross DJ, Rehemtulla A, Ross BD, Chenevert TL. Functional diffusion map as an early imaging biomarker for high-grade glioma: correlation with conventional radiologic response and overall survival. J. Clin. Oncol. 2008; 26(20): 3387–3394.
94. Padhani AR, Liu G, Mu-Koh D, Chenevert TL, Thoeny HC, Takahara T, Dzik-Jurasz A, Ross BD, Van Cauteren M, Collins D, Hammoud DA, Rustin GJ, Taouli B, Choyke PL. Diffusion-weighted magnetic resonance imaging as a cancer biomarker: consensus and recommendations. Neoplasia 2009; 11(2): 102–125.
95. Delakis I, Moore EM, Leach MO, De Wilde JP. Developing a quality control protocol for diffusion imaging on a clinical MRI system. Phys. Med. Biol. 2004; 49(8): 1409–1422.
96. Laubach HJ, Jakob PM, Loevblad KO, Baird AE, Bovo MP, Edelman RR, Warach S. A phantom for diffusion-weighted imaging of acute stroke. J. Magn. Reson. Imaging 1998; 8(6): 1349–1354.
97. Tofts PS, Lloyd D, Clark CA, Barker GJ, Parker GJ, McConville P, Baldock C, Pope JM. Test liquids for quantitative MRI measurements of self-diffusion coefficient in vivo. Magn. Reson. Med. 2000; 43(3): 368–374.
98. Chenevert TL, Galban CJ, Ivancevic MK, Rohrer SE, Londy FJ, Kwee TC, Meyer CR, Johnson TD, Rehemtulla A, Ross BD. Diffusion coefficient measurement using a temperature-controlled fluid for quality control in multicenter studies. J. Magn. Reson. Imaging 2011; 34(4): 983–987.
99. Simpson JH, Carr HY. Diffusion and nuclear spin relaxation in water. Phys. Rev. 1958; 111: 1201–1202.

100. Belli G, Busoni S, Ciccarone A, Coniglio A, Esposito M, Giannelli M, Mazzoni LN, Nocetti L, Sghedoni R, Tarducci R, Zatelli G, Anoja RA, Belmonte G, Bertolino N, Betti M, Biagini C, Ciarmatori A, Cretti F, Fabbri E, Fedeli L, Filice S, Fulcheri CP, Gasperi C, Mangili PA, Mazzocchi S, Meliado G, Morzenti S, Noferini L, Oberhofer N, Orsingher L, Paruccini N, Princigalli G, Quattrocchi M, Rinaldi A, Scelfo D, Freixas GV, Tenori L, Zucca I, Luchinat C, Gori C, Gobbi G, Italian Association of Physics in Medicine Working Group on MRI. Quality assurance multicenter comparison of different MR scanners for quantitative diffusion-weighted imaging. J. Magn. Reson. Imaging 2015. doi: 10.1002/jmri.24956. [Epub ahead of print]
101. Malyarenko D, Galban CJ, Londy FJ, Meyer CR, Johnson TD, Rehemtulla A, Ross BD, Chenevert TL. Multi-system repeatability and reproducibility of apparent diffusion coefficient measurement using an ice–water phantom. J. Magn. Reson. Imaging 2013; 37(5): 1238–1246.
102. Kakite S, Dyvorne H, Besa C, Cooper N, Facciuto M, Donnerhack C, Taouli B. Hepatocellular carcinoma: short-term reproducibility of apparent diffusion coefficient and intravoxel incoherent motion parameters at 3.0T. J. Magn. Reson. Imaging, 2015; 41(1): 149–156.
103. Bernardin L, Douglas NH, Collins DJ, Giles SL, O'Flynn EA, Orton M, deSouza NM. Diffusion-weighted magnetic resonance imaging for assessment of lung lesions: repeatability of the apparent diffusion coefficient measurement. Eur. Radiol. 2014; 24(2): 502–511.
104. Intven M, Reerink O, Philippens ME. Repeatability of diffusion-weighted imaging in rectal cancer. J. Magn. Reson. Imaging 2014; 40(1): 146–150.
105. Galban CJ, Ma B, Malyarenko D, Pickles MD, Heist K, Henry NL, Schott AF, Neal CH, Hylton NM, Rehemtulla A, Johnson TD, Meyer CR, Chenevert TL, Turnbull LW, Ross BD. Multi-site clinical evaluation of DW-MRI as a treatment response metric for breast cancer patients undergoing neoadjuvant chemotherapy. PloS One 2015; 10(3): e0122151.
106. Heo S, Cho HJ, Jeon IS. A case of posterior reversible encephalopathy syndrome in a child with myelodysplastic syndrome following allogenic bone marrow transplantation. Pediatr. Hematol. Oncol. 2010; 27(1): 59–64.
107. Huang RY, Neagu MR, Reardon DA, Wen PY. Pitfalls in the neuroimaging of glioblastoma in the era of antiangiogenic and immuno/targeted therapy – detecting illusive disease, defining response. Frontiers Neurol. 2015; 6: 33.
108. Rygh CB, Wang J, Thuen M, Gras Navarro A, Huuse EM, Thorsen F, Poli A, Zimmer J, Haraldseth O, Lie SA, Enger PO, Chekenya M. Dynamic contrast enhanced MRI detects early response to adoptive NK cellular immunotherapy targeting the NG2 proteoglycan in a rat model of glioblastoma. PloS One 2014; 9(9): e108414.
109. McDonald K, Sebire NJ, Anderson J, Olsen OE. Patterns of shift in ADC distributions in abdominal tumours during chemotherapy-feasibility study. Pediatr. Radiol. 2011; 41(1): 99–106.
110. Wai Y, Chu J, Wang C, Lin Y, Lin G, Wan Y, Wang J. An integrated diffusion map for the analysis of diffusion properties: a feasibility study in patients with acoustic neuroma. Acad. Radiol. 2009; 16(4): 428–434.
111. Nakayama T, Yoshida S, Fujii Y, Koga F, Saito K, Masuda H, Kobayashi T, Kawakami S, Kihara K. Use of diffusion-weighted MRI in monitoring response of lymph node metastatic bladder cancer treated with chemotherary. Nihon Hinyokika Gakkai zasshi [Jpn. J. Urol.] 2008; 99(7): 737–741.
112. Yoshida S, Koga F, Kawakami S, Ishii C, Tanaka H, Numao N, Sakai Y, Saito K, Masuda H, Fujii Y, Kihara K. Initial experience of diffusion-weighted magnetic resonance imaging to assess therapeutic response to induction chemoradiotherapy against muscle-invasive bladder cancer. Urology 2010; 75(2): 387–391.
113. Ballon D, Watts R, Dyke JP, Lis E, Morris MJ, Scher HI, Ulug AM, Jakubowski AA. Imaging therapeutic response in human bone marrow using rapid whole-body MRI. Magn. Reson. Med. 2004; 52(6): 1234–1238.
114. Armitage PA, Schwindack C, Bastin ME, Whittle IR. Quantitative assessment of intracranial tumor response to dexamethasone using diffusion, perfusion and permeability magnetic resonance imaging. Magn. Reson. Imaging 2007; 25(3): 303–310.
115. Bastin ME, Delgado M, Whittle IR, Cannon J, Wardlaw JM. The use of diffusion tensor imaging in quantifying the effect of dexamethasone on brain tumours. Neuroreport 1999; 10(7): 1385–1391.
116. Huang CF, Chiou SY, Wu MF, Tu HT, Liu WS, Chuang JC. Apparent diffusion coefficients for evaluation of the response of brain tumors treated by gamma knife surgery. J. Neurosurg. 2010; 113-(Suppl): 97–104.
117. Mardor Y, Roth Y, Lidar Z, Jonas T, Pfeffer R, Maier SE, Faibel M, Nass D, Hadani M, Orenstein A, Cohen JS, Ram Z. Monitoring response to convection-enhanced taxol delivery in brain tumor patients using diffusion-weighted magnetic resonance imaging. Cancer Res. 2001; 61(13): 4971–4973.
118. Mardor Y, Roth Y, Ochershvilli A, Spiegelmann R, Tichler T, Daniels D, Maier SE, Nissim O, Ram Z, Baram J, Orenstein A, Pfeffer R. Pretreatment prediction of brain tumors' response to radiation therapy using high b-value diffusion-weighted MRI. Neoplasia 2004; 6(2): 136–142.
119. Mardor Y, Pfeffer R, Spiegelmann R, Roth Y, Maier SE, Nissim O, Berger R, Glicksman A, Baram J, Orenstein A, Cohen JS, Tichler T. Early detection of response to radiation therapy in patients with brain malignancies using conventional and high b-value diffusion-weighted magnetic resonance imaging. J. Clin. Oncol. 2003; 21(6): 1094–1100.
120. Tomura N, Narita K, Izumi J, Suzuki A, Anbai A, Otani T, Sakuma I, Takahashi S, Mizoi K, Watarai J. Diffusion changes in a tumor and peritumoral tissue after stereotactic irradiation for brain tumors: possible prediction of treatment response. J. Comput. Assist. Tomogr. 2006; 30(3): 496–500.
121. Goldman M, Boxerman JL, Rogg JM, Noren G. Utility of apparent diffusion coefficient in predicting the outcome of gamma knife-treated brain metastases prior to changes in tumor volume: a preliminary study. J. Neurosurg 2006; 105(Suppl): 175–182.
122. Gupta A, Young RJ, Karimi S, Sood S, Zhang Z, Mo Q, Gutin PH, Holodny AI, Lassman AB. Isolated diffusion restriction precedes the development of enhancing tumor in a subset of patients with glioblastoma. Am. J. Neuroradiol. 2011; 32(7): 1301–1306.
123. Hattingen E, Jurcoane A, Bahr O, Rieger J, Magerkurth J, Anti S, Steinbach JP, Pilatus U. Bevacizumab impairs oxidative energy metabolism and shows antitumoral effects in recurrent glioblastomas: a $^{31}P/^{1}H$ MRSI and quantitative magnetic resonance imaging study. Neuro-oncology 2011; 13(12): 1349–1363.
124. Pope WB, Lai A, Mehta R, Kim HJ, Qiao J, Young JR, Xue X, Goldin J, Brown MS, Nghiemphu PL, Tran A, Cloughesy TF. Apparent diffusion coefficient histogram analysis stratifies progression-free survival in newly diagnosed bevacizumab-treated glioblastoma. Am. J. Neuroradiol. 2011; 32(5): 882–889.
125. Vrabec M, Van Cauter S, Himmelreich U, Van Gool SW, Sunaert S, De Vleeschouwer S, Suput D, Demaerel P. MR perfusion and diffusion imaging in the follow-up of recurrent glioblastoma treated with dendritic cell immunotherapy: a pilot study. Neuroradiology 2011; 53(10): 721–731.
126. Yamasaki F, Kurisu K, Aoki T, Yamanaka M, Kajiwara Y, Watanabe Y, Takayasu T, Akiyama Y, Sugiyama K. Advantages of high b-value diffusion-weighted imaging to diagnose pseudo-responses in patients with recurrent glioma after bevacizumab treatment. Eur. J. Radiol. 2012; 81(10): 2805–2810.
127. Galban CJ, Chenevert TL, Meyer CR, Tsien C, Lawrence TS, Hamstra DA, Junck L, Sundgren PC, Johnson TD, Galban S, Sebolt-Leopold JS, Rehemtulla A, Ross BD. Prospective analysis of parametric response map-derived MRI biomarkers: identification of early and distinct glioma response patterns not predicted by standard radiographic assessment. Clin. Cancer Res. 2011; 17(14): 4751–4760.
128. Nowosielski M, Recheis W, Goebel G, Guler O, Tinkhauser G, Kostron H, Schocke M, Gotwald T, Stockhammer G, Hutterer M. ADC histograms predict response to anti-angiogenic therapy in patients with recurrent high-grade glioma. Neuroradiology 2011; 53(4): 291–302.
129. Prabhu SP, Ng S, Vajapeyam S, Kieran MW, Pollack IF, Geyer R, Haas-Kogan D, Boyett JM, Kun L, Poussaint TY. DTI assessment of the brainstem white matter tracts in pediatric BSG before and after therapy: a report from the Pediatric Brain Tumor Consortium. Child Nerv. Syst. 2011; 27(1): 11–18.
130. Ringelstein A, Turowski B, Gizewski ER, Schroeteler J, Rapp M, Saleh A, Lanzman RS, Mathys C, Sabel M, Modder U. [Evaluation of ADC mapping as an early predictor for tumor response to chemotherapy in recurrent glioma treated with bevacizumab/irinotecan: proof of principle]. RoFo: Fortschr. Gebiete Rontgenstrahlen Nuklearmedizin 2010; 182(10): 868–872.

131. Chen HJ, Panigrahy A, Dhall G, Finlay JL, Nelson MD Jr., Bluml S. Apparent diffusion and fractional anisotropy of diffuse intrinsic brain stem gliomas. Am. J. Neuroradiol. 2010; 31(10): 1879–1885.
132. Jain R, Scarpace LM, Ellika S, Torcuator R, Schultz LR, Hearshen D, Mikkelsen T. Imaging response criteria for recurrent gliomas treated with bevacizumab: role of diffusion weighted imaging as an imaging biomarker. J. Neuro-oncol. 2010; 96(3): 423–431.
133. Seshadri M, Ciesielski MJ. MRI-based characterization of vascular disruption by 5,6-dimethylxanthenone-acetic acid in gliomas. J. Cerebr. Blood Flow Metab. 2009; 29(8): 1373–1382.
134. Jager HR, Waldman AD, Benton C, Fox N, Rees J. Differential chemosensitivity of tumor components in a malignant oligodendroglioma: assessment with diffusion-weighted, perfusion-weighted, and serial volumetric MR imaging. Am. J. Neuroradiol. 2005; 26(2): 274–278.
135. Lidar Z, Mardor Y, Jonas T, Pfeffer R, Faibel M, Nass D, Hadani M, Ram Z. Convection-enhanced delivery of paclitaxel for the treatment of recurrent malignant glioma: a phase I/II clinical study. J. Neurosurg. 2004; 100(3): 472–479.
136. Lin YC, Wang CC, Wai YY, Wan YL, Ng SH, Chen YL, Liu HL, Wang JJ. Significant temporal evolution of diffusion anisotropy for evaluating early response to radiosurgery in patients with vestibular schwannoma: findings from functional diffusion maps. Am. J. Neuroradiol. 2010; 31(2): 269–274.
137. Schubert MI, Wilke M, Muller-Weihrich S, Auer DP. Diffusion-weighted magnetic resonance imaging of treatment-associated changes in recurrent and residual medulloblastoma: preliminary observations in three children. Acta Radiol. 2006; 47(10): 1100–1104.
138. Sinha S, Bastin ME, Whittle IR. Rapid clinical deterioration in a patient with multi-focal glioma despite corticosteroid therapy: a quantitative MRI study. Br. J. Neurosurg. 2003; 17(6): 537–540 discussion 540.
139. Arlinghaus LR, Li X, Rahman AR, Welch EB, Xu L, Gore JC, Yankeelov TE. On the relationship between the apparent diffusion coefficient and extravascular extracellular volume fraction in human breast cancer. Magn. Reson. Imaging 2011; 29(5): 630–638.
140. Belli P, Costantini M, Ierardi C, Bufi E, Amato D, Mule A, Nardone L, Terribile D, Bonomo L. Diffusion-weighted imaging in evaluating the response to neoadjuvant breast cancer treatment. Breast J. 2011; 17(6): 610–619.
141. Fangberget A, Nilsen LB, Hole KH, Holmen MM, Engebraaten O, Naume B, Smith HJ, Olsen DR, Seierstad T. Neoadjuvant chemotherapy in breast cancer-response evaluation and prediction of response to treatment using dynamic contrast-enhanced and diffusion-weighted MR imaging. Eur. Radiol. 2011; 21(6): 1188–1199.
142. Jensen LR, Garzon B, Heldahl MG, Bathen TF, Lundgren S, Gribbestad IS. Diffusion-weighted and dynamic contrast-enhanced MRI in evaluation of early treatment effects during neoadjuvant chemotherapy in breast cancer patients. J. Magn. Reson. Imaging 2011; 34(5): 1099–1109.
143. Jinming X, Qi Z, Xiaoming Z, Jianming T. Primary non-Hodgkin's lymphoma of the breast: mammography, ultrasound, MRI and pathologic findings. Future Oncol. 2012; 8(1): 105–109.
144. Kawamura M, Satake H, Ishigaki S, Nishio A, Sawaki M, Naganawa S. Early prediction of response to neoadjuvant chemotherapy for locally advanced breast cancer using MRI. Nagoya J. Med. Sci. 2011; 73(3–4): 147–156.
145. Li XR, Cheng LQ, Liu M, Zhang YJ, Wang JD, Zhang AL, Song X, Li J, Zheng YQ, Liu L. DW-MRI ADC values can predict treatment response in patients with locally advanced breast cancer undergoing neoadjuvant chemotherapy. Med. Oncol. 2012; 29(2): 425–431.
146. Park SH, Moon WK, Cho N, Chang JM, Im SA, Park IA, Kang KW, Han W, Noh DY. Comparison of diffusion-weighted MR imaging and FDG PET/CT to predict pathological complete response to neoadjuvant chemotherapy in patients with breast cancer. Eur. Radiol. 2012; 22(1): 18–25.
147. Wang XH, Peng WJ, Tan HN, Xin C, Gu YJ, Tang F, Mao J. Value of diffusion weighted imaging (DWI) in evaluating early response to neoadjuvant chemotherapy in locally advanced breast cancer. Zhonghua zhong liu za zhi [Chin. J. Oncol.] 2010; 32(5): 377–381.
148. Buijs M, Kamel IR, Vossen JA, Georgiades CS, Hong K, Geschwind JF. Assessment of metastatic breast cancer response to chemoembolization with contrast agent enhanced and diffusion-weighted MR imaging. J. Vasc. Intervent. Radiol. 2007; 18(8): 957–963.
149. Ma B, Meyer CR, Pickles MD, Chenevert TL, Bland PH, Galban CJ, Rehemtulla A, Turnbull LW, Ross BD. Voxel-by-voxel functional diffusion mapping for early evaluation of breast cancer treatment. Proc. Conf. Inform. Process. Med. Imaging 2009; 21: 276–287.
150. Nilsen L, Fangberget A, Geier O, Olsen DR, Seierstad T. Diffusion-weighted magnetic resonance imaging for pretreatment prediction and monitoring of treatment response of patients with locally advanced breast cancer undergoing neoadjuvant chemotherapy. Acta Oncol. 2010; 49(3): 354–360.
151. Tozaki M, Oyama Y, Fukuma E. Preliminary study of early response to neoadjuvant chemotherapy after the first cycle in breast cancer: comparison of ^{1}H magnetic resonance spectroscopy with diffusion magnetic resonance imaging. Jpn. J. Radiol. 2010; 28(2): 101–109.
152. Manton DJ, Chaturvedi A, Hubbard A, Lind MJ, Lowry M, Maraveyas A, Pickles MD, Tozer DJ, Turnbull LW. Neoadjuvant chemotherapy in breast cancer: early response prediction with quantitative MR imaging and spectroscopy. Br. J. Cancer 2006; 94(3): 427–435.
153. Harry VN, Semple SI, Gilbert FJ, Parkin DE. Diffusion-weighted magnetic resonance imaging in the early detection of response to chemoradiation in cervical cancer. Gynecol. Oncol. 2008; 111(2): 213–220.
154. Levy A, Caramella C, Chargari C, Medjhoul A, Rey A, Zareski E, Boulet B, Bidault F, Dromain C, Balleyguier C. Accuracy of diffusion-weighted echo-planar MR imaging and ADC mapping in the evaluation of residual cervical carcinoma after radiation therapy. Gynecol. Oncol. 2011; 123(1): 110–115.
155. Liu Y, Bai R, Sun H, Liu H, Zhao X, Li Y. Diffusion-weighted imaging in predicting and monitoring the response of uterine cervical cancer to combined chemoradiation. Clin. Radiol. 2009; 64(11): 1067–1074.
156. Matge G. Anterior interbody fusion with the BAK-cage in cervical spondylosis. Acta Neurochirurg. 1998; 140(1): 1–8.
157. McVeigh PZ, Syed AM, Milosevic M, Fyles A, Haider MA. Diffusion-weighted MRI in cervical cancer. Eur. Radiol. 2008; 18(5): 1058–1064.
158. Rizzo S, Summers P, Raimondi S, Belmonte M, Maniglio M, Landoni F, Colombo N, Bellomi M. Diffusion-weighted MR imaging in assessing cervical tumour response to nonsurgical therapy. Radiol. Med. 2011; 116(5): 766–780.
159. Zhang Y, Chen JY, Xie CM, Mo YX, Liu XW, Liu Y, Wu PH. Diffusion-weighted magnetic resonance imaging for prediction of response of advanced cervical cancer to chemoradiation. J. Comput. Assist. Tomogr. 2011; 35(1): 102–107.
160. Zhang Y, Liang BL, Gao L, Ye RX, Shen J, Zhong JL. [Diffusion weighted imaging features of normal uterine cervix and cervical carcinoma]. Ai zheng = Aizheng [Chin. J. Cancer] 2007; 26(5): 508–512.
161. Buijs M, Vossen JA, Hong K, Georgiades CS, Geschwind JF, Kamel IR. Chemoembolization of hepatic metastases from ocular melanoma: assessment of response with contrast-enhanced and diffusion-weighted MRI. Am. J. Roentgenol. 2008; 191(1): 285–289.
162. Politi LS, Forghani R, Godi C, Resti AG, Ponzoni M, Bianchi S, Iadanza A, Ambrosi A, Falini A, Ferreri AJ, Curtin HD, Scotti G. Ocular adnexal lymphoma: diffusion-weighted MR imaging for differential diagnosis and therapeutic monitoring. Radiology 2010; 256(2): 565–574.
163. Hecht EM, Do RK, Kang SK, Bennett GL, Babb JS, Clark TW. Diffusion-weighted imaging for prediction of volumetric response of leiomyomas following uterine artery embolization: a preliminary study. J. Magn. Reson. Imaging 2011; 33(3): 641–646.
164. Saraiya B, Chugh R, Karantza V, Mehnert J, Moss RA, Savkina N, Stein MN, Baker LH, Chenevert T, Poplin EA. Phase I study of gemcitabine, docetaxel and imatinib in refractory and relapsed solid tumors. Invest. New Drugs 2012; 30(1): 258–265.
165. Vossen JA, Kamel IR, Buijs M, Liapi E, Georgiades CS, Hong K, Geschwind JF. Role of functional magnetic resonance imaging in assessing metastatic leiomyosarcoma response to chemoembolization. J. Comput. Assist. Tomogr. 2008; 32(3): 347–352.
166. Choi SA, Lee SS, Jung IH, Kim HA, Byun JH, Lee MG. The effect of gadoxetic acid enhancement on lesion detection and characterisation using T(2) weighted imaging and diffusion weighted imaging of the liver. Br. J. Radiol. 2012; 85(1009): 29–36.
167. Dudeck O, Zeile M, Wybranski C, Schulmeister A, Fischbach F, Pech M, Wieners G, Ruhl R, Grosser O, Amthauer H, Ricke J. Early prediction of anticancer effects with diffusion-weighted MR imaging in patients with colorectal liver metastases following

selective internal radiotherapy. Eur. Radiol. 2010; 20(11): 2699–2706.
168. Koh DM, Scurr E, Collins D, Kanber B, Norman A, Leach MO, Husband JE. Predicting response of colorectal hepatic metastasis: value of pretreatment apparent diffusion coefficients. Am. J. Roentgenol. 2007; 188(4): 1001–1008.
169. Wybranski C, Zeile M, Lowenthal D, Fischbach F, Pech M, Rohl FW, Gademann G, Ricke J, Dudeck O. Value of diffusion weighted MR imaging as an early surrogate parameter for evaluation of tumor response to high-dose-rate brachytherapy of colorectal liver metastases. Radiat. Oncol. 2011; 6(1): 43.
170. Zhang Y, Zhao J, Guo D, Zhong W, Ran L. Evaluation of short-term response of high intensity focused ultrasound ablation for primary hepatic carcinoma: utility of contrast-enhanced MRI and diffusion-weighted imaging. Eur. J. Radiol. 2011; 79(3): 347–352.
171. Duke E, Deng J, Ibrahim SM, Lewandowski RJ, Ryu RK, Sato KT, Miller FH, Kulik L, Mulcahy MF, Larson AC, Salem R, Omary RA. Agreement between competing imaging measures of response of hepatocellular carcinoma to yttrium-90 radioembolization. J. Vasc. Intervent. Radiol. 2010; 21(4): 515–521.
172. Kubota K, Yamanishi T, Itoh S, Murata Y, Miyatake K, Yasunami H, Morio K, Hamada N, Nishioka A, Ogawa Y. Role of diffusion-weighted imaging in evaluating therapeutic efficacy after transcatheter arterial chemoembolization for hepatocellular carcinoma. Oncol. Rep. 2010; 24(3): 727–732.
173. Liapi E, Geschwind JF, Vossen JA, Buijs M, Georgiades CS, Bluemke DA, Kamel IR. Functional MRI evaluation of tumor response in patients with neuroendocrine hepatic metastasis treated with transcatheter arterial chemoembolization. Am. J. Roentgenol. 2008; 190(1): 67–73.
174. Eccles CL, Haider EA, Haider MA, Fung S, Lockwood G, Dawson LA. Change in diffusion weighted MRI during liver cancer radiotherapy: preliminary observations. Acta Oncol. 2009; 48(7): 1034–1043.
175. Schraml C, Schwenzer NF, Martirosian P, Bitzer M, Lauer U, Claussen CD, Horger M. Diffusion-weighted MRI of advanced hepatocellular carcinoma during sorafenib treatment: initial results. Am. J. Roentgenol. 2009; 193(4): W301–W307.
176. Yuan Z, Ye XD, Dong S, Xu LC, Xu XY, Liu SY, Xiao XS. Role of magnetic resonance diffusion-weighted imaging in evaluating response after chemoembolization of hepatocellular carcinoma. Eur. J. Radiol. 2010; 75(1): e9–e14.
177. Anzidei M, Napoli A, Zaccagna F, Cartocci G, Saba L, Menichini G, Cavallo Marincola B, Marotta E, Di Mare L, Catalano C, Passariello R. Liver metastases from colorectal cancer treated with conventional and antiangiogenetic chemotherapy: evaluation with liver computed tomography perfusion and magnetic resonance diffusion-weighted imaging. J. Comput. Assist. Tomogr. 2011; 35(6): 690–696.
178. Bonekamp S, Shen J, Salibi N, Lai HC, Geschwind J, Kamel IR. Early response of hepatic malignancies to locoregional therapy – value of diffusion-weighted magnetic resonance imaging and proton magnetic resonance spectroscopy. J. Comput. Assist. Tomogr. 2011; 35(2): 167–173.
179. Yuan Z, Ye XD, Dong S, Xu LC, Sun ZC, Xiao XS. [Water mobility of diffusion MRI in prediction of response to chemoembolization in liver cancer]. Zhonghua zhong liu za zhi [Chin. J. Oncol.] 2009; 31(4): 293–297.
180. Chung JC, Naik NK, Lewandowski RJ, Deng J, Mulcahy MF, Kulik LM, Sato KT, Ryu RK, Salem R, Larson AC, Omary RA. Diffusion-weighted magnetic resonance imaging to predict response of hepatocellular carcinoma to chemoembolization. World J. Gastroenterol. 2010; 16(25): 3161–3167.
181. El-Khouli RH, Geschwind JF, Bluemke DA, Kamel IR. Solitary fibrous tumor of the liver: magnetic resonance imaging evaluation and treatment with transarterial chemoembolization. J. Comput. Assist. Tomogr. 2008; 32(5): 769–771.
182. Chang Q, Wu N, Ouyang H, Huang Y. Diffusion-weighted magnetic resonance imaging of lung cancer at 3.0 T: a preliminary study on monitoring diffusion changes during chemoradiation therapy. Clin. Imaging 2012; 36(2): 98–103.
183. Ohno Y, Koyama H, Yoshikawa T, Matsumoto K, Aoyama N, Onishi Y, Sugimura K. Diffusion-weighted MRI versus ^{18}F-FDG PET/CT: performance as predictors of tumor treatment response and patient survival in patients with non-small cell lung cancer receiving chemoradiotherapy. Am. J. Roentgenol. 2012; 198(1): 75–82.
184. Okuma T, Matsuoka T, Yamamoto A, Hamamoto S, Nakamura K, Inoue Y. Assessment of early treatment response after CT-guided radiofrequency ablation of unresectable lung tumours by diffusion-weighted MRI: a pilot study. Br. J. Radiol. 2009; 82(984): 989–994.
185. Zhou R, Yu T, Feng C, Ma L, Wang Y, Li W, Wang Y. [Diffusion-weighted imaging for assessment of lung cancer response to chemotherapy]. Zhongguo fei ai za zhi [Chin. J. Lung Cancer] 2011; 14(3): 256–260.
186. Lin C, Itti E, Luciani A, Zegai B, Lin SJ, Kuhnowski F, Pigneur F, Gaillard I, Paone G, Meignan M, Haioun C, Rahmouni A. Whole-body diffusion-weighted imaging with apparent diffusion coefficient mapping for treatment response assessment in patients with diffuse large B-cell lymphoma: pilot study. Invest. Radiol. 2011; 46(5): 341–349.
187. Marzolini M, Wong WL, Ardeshna K, Padhani A, D'Sa S. Diffusion-weighted MRI compared to FDG PET-CT in the staging and response assessment of Hodgkin lymphoma. Br. J. Haematol. 2012; 156(5): 557.
188. Wu X, Kellokumpu-Lehtinen PL, Pertovaara H, Korkola P, Soimakallio S, Eskola H, Dastidar P. Diffusion-weighted MRI in early chemotherapy response evaluation of patients with diffuse large B-cell lymphoma—a pilot study: comparison with 2-deoxy-2-fluoro-D-glucose-positron emission tomography/computed tomography. NMR Biomed. 2011; 24(10): 1181–1190.
189. Fenchel M, Konaktchieva M, Weisel K, Kraus S, Claussen CD, Horger M. Response assessment in patients with multiple myeloma during antiangiogenic therapy using arterial spin labeling and diffusion-weighted imaging: a feasibility study. Acad. Radiol. 2010; 17(11): 1326–1323.
190. Horger M, Weisel K, Horger W, Mroue A, Fenchel M, Lichy M. Whole-body diffusion-weighted MRI with apparent diffusion coefficient mapping for early response monitoring in multiple myeloma: preliminary results. Am. J. Roentgenol. 2011; 196(6): W790–W795.
191. Kyriazi S, Collins DJ, Messiou C, Pennert K, Davidson RL, Giles SL, Kaye SB, Desouza NM. Metastatic ovarian and primary peritoneal cancer: assessing chemotherapy response with diffusion-weighted MR imaging—value of histogram analysis of apparent diffusion coefficients. Radiology 2011; 261(1): 182–192.
192. Kyriazi S, Nye E, Stamp G, Collins DJ, Kaye SB, deSouza NM. Value of diffusion-weighted imaging for assessing site-specific response of advanced ovarian cancer to neoadjuvant chemotherapy: correlation of apparent diffusion coefficients with epithelial and stromal densities on histology. Cancer Biomark 2010; 7(4): 201–210.
193. Sala E, Kataoka MY, Priest AN, Gill AB, McLean MA, Joubert I, Graves MJ, Crawford RA, Jimenez-Linan M, Earl HM, Hodgkin C, Griffiths JR, Lomas DJ, Brenton JD. Advanced ovarian cancer: multiparametric MR imaging demonstrates response- and metastasis-specific effects. Radiology 2012; 263(1): 149–159.
194. Niwa T, Ueno M, Ohkawa S, Yoshida T, Doiuchi T, Ito K, Inoue T. Advanced pancreatic cancer: the use of the apparent diffusion coefficient to predict response to chemotherapy. Br. J. Radiol. 2009; 82(973): 28–34.
195. Barrett T, Gill AB, Kataoka MY, Priest AN, Joubert I, McLean MA, Graves MJ, Stearn S, Lomas DJ, Griffiths JR, Neal D, Gnanapragasam VJ, Sala E. DCE and DW MRI in monitoring response to androgen deprivation therapy in patients with prostate cancer: a feasibility study. Magn. Reson. Med. 2012; 67(3): 778–785.
196. Messiou C, Collins DJ, Giles S, de Bono JS, Bianchini D, de Souza NM. Assessing response in bone metastases in prostate cancer with diffusion weighted MRI. Eur. Radiol. 2011; 21(10): 2169–2177.
197. Nemoto K, Tateishi T, Ishidate T. Changes in diffusion-weighted images for visualizing prostate cancer during antiandrogen therapy: preliminary results. Urol. Int. 2010; 85(4): 421–426.
198. Song I, Kim CK, Park BK, Park W. Assessment of response to radiotherapy for prostate cancer: value of diffusion-weighted MRI at 3 T. Am. J. Roentgenol. 2010; 194(6): W477–W482.
199. Curvo-Semedo L, Lambregts DM, Maas M, Thywissen T, Mehsen RT, Lammering G, Beets GL, Caseiro-Alves F, Beets-Tan RG. Rectal cancer: assessment of complete response to preoperative combined radiation therapy with chemotherapy—conventional MR volumetry versus diffusion-weighted MR imaging. Radiology 2011; 260(3): 734–743.
200. Jang KM, Kim SH, Choi D, Lee SJ, Park MJ, Min K. Pathological correlation with diffusion restriction on diffusion-weighted imaging in

patients with pathological complete response after neoadjuvant chemoradiation therapy for locally advanced rectal cancer: preliminary results. Br. J. Radiol. 2012; 85(1017): e566–e572.
201. Kim SH, Lee JY, Lee JM, Han JK, Choi BI. Apparent diffusion coefficient for evaluating tumour response to neoadjuvant chemoradiation therapy for locally advanced rectal cancer. Eur. Radiol. 2011; 21(5): 987–995.
202. Lambrecht M, Vandecaveye V, De Keyzer F, Roels S, Penninckx F, Van Cutsem E, Filip C, Haustermans K. Value of diffusion-weighted magnetic resonance imaging for prediction and early assessment of response to neoadjuvant radiochemotherapy in rectal cancer: preliminary results. Int. J. Radiat. Oncol. Biol. Phys. 2012; 82(2): 863–870.
203. Lambregts DM, Beets GL, Maas M, Curvo-Semedo L, Kessels AG, Thywissen T, Beets-Tan RG. Tumour ADC measurements in rectal cancer: effect of ROI methods on ADC values and interobserver variability. Eur. Radiol. 2011; 21(12): 2567–2574.
204. Lambregts DM, Vandecaveye V, Barbaro B, Bakers FC, Lambrecht M, Maas M, Haustermans K, Valentini V, Beets GL, Beets-Tan RG. Diffusion-weighted MRI for selection of complete responders after chemoradiation for locally advanced rectal cancer: a multicenter study. Ann. Surg. Oncol. 2011; 18(8): 2224–2231.
205. Seehaus A, Vacaro C, Ocantos J, Varela A, Savluk L, Ojea Quintana G, Rossi G, Weimbaur V, Pablo Santino J, Garcia-Monaco R. [Diffusion-weighted MR imaging in patients with rectal cancer: our initial experience]. Acta Gastroenterol. Latinoam. 2011; 41(3): 199–207.
206. DeVries AF, Kremser C, Hein PA, Griebel J, Krezcy A, Ofner D, Pfeiffer KP, Lukas P, Judmaier W. Tumor microcirculation and diffusion predict therapy outcome for primary rectal carcinoma. Int. J. Radiat. Oncol. Biol. Phys. 2003; 56(4): 958–965.
207. Lambrecht M, Deroose C, Roels S, Vandecaveye V, Penninckx F, Sagaert X, van Cutsem E, de Keyzer F, Haustermans K. The use of FDG-PET/CT and diffusion-weighted magnetic resonance imaging for response prediction before, during and after preoperative chemoradiotherapy for rectal cancer. Acta Oncol. 2010; 49(7): 956–963.
208. Bajpai J, Gamnagatti S, Kumar R, Sreenivas V, Sharma MC, Khan SA, Rastogi S, Malhotra A, Safaya R, Bakhshi S. Role of MRI in osteosarcoma for evaluation and prediction of chemotherapy response: correlation with histological necrosis. Pediatr. Radiol. 2011; 41(4): 441–450.
209. Baunin C, Schmidt G, Baumstarck K, Bouvier C, Gentet JC, Aschero A, Ruocco A, Bourliere B, Gorincour G, Desvignes C, Colavolpe N, Bollini G, Auqier P, Petit P. Value of diffusion-weighted images in differentiating mid-course responders to chemotherapy for osteosarcoma compared to the histological response: preliminary results. Skel. Radiol. 2012; 41(9): 1141–1149.
210. Dudeck O, Zeile M, Pink D, Pech M, Tunn PU, Reichardt P, Ludwig WD, Hamm B. Diffusion-weighted magnetic resonance imaging allows monitoring of anticancer treatment effects in patients with soft-tissue sarcomas. J. Magn. Reson. Imaging 2008; 27(5): 1109–1113.
211. Oka K, Yakushiji T, Sato H, Hirai T, Yamashita Y, Mizuta H. The value of diffusion-weighted imaging for monitoring the chemotherapeutic response of osteosarcoma: a comparison between average apparent diffusion coefficient and minimum apparent diffusion coefficient. Skel. Radiol. 2010; 39(2): 141–146.
212. Uhl M, Saueressig U, Koehler G, Kontny U, Niemeyer C, Reichardt W, Ilyasof K, Bley T, Langer M. Evaluation of tumour necrosis during chemotherapy with diffusion-weighted MR imaging: preliminary results in osteosarcomas. Pediatr. Radiol. 2006; 36(12): 1306–1311.
213. Einarsdottir H, Karlsson M, Wejde J, Bauer HC. Diffusion-weighted MRI of soft tissue tumours. Eur. Radiol. 2004; 14(6): 959–963.
214. Koh DM, Blackledge M, Collins DJ, Padhani AR, Wallace T, Wilton B, Taylor NJ, Stirling JJ, Sinha R, Walicke P, Leach MO, Judson I, Nathan P. Reproducibility and changes in the apparent diffusion coefficients of solid tumours treated with combretastatin A4 phosphate and bevacizumab in a two-centre phase I clinical trial. Eur. Radiol. 2009; 19(11): 2728–2738.
215. Dirix P, Vandecaveye V, De Keyzer F, Stroobants S, Hermans R, Nuyts S. Dose painting in radiotherapy for head and neck squamous cell carcinoma: value of repeated functional imaging with (18)F-FDG PET, (18)F-fluoromisonidazole PET, diffusion-weighted MRI, and dynamic contrast-enhanced MRI. J. Nucl. Med. 2009; 50(7): 1020–1027.
216. King AD, Mo FK, Yu KH, Yeung DK, Zhou H, Bhatia KS, Tse GM, Vlantis AC, Wong JK, Ahuja AT. Squamous cell carcinoma of the head and neck: diffusion-weighted MR imaging for prediction and monitoring of treatment response. Eur. Radiol. 2010; 20(9): 2213–2220.
217. Vandecaveye V, Dirix P, De Keyzer F, de Beeck KO, Vander Poorten V, Roebben I, Nuyts S, Hermans R. Predictive value of diffusion-weighted magnetic resonance imaging during chemoradiotherapy for head and neck squamous cell carcinoma. Eur. Radiol. 2010; 20(7): 1703–1714.
218. Vandecaveye V, Dirix P, De Keyzer F, Op de Beeck K, Vander Poorten V, Hauben E, Lambrecht M, Nuyts S, Hermans R, Levy A. Diffusion-weighted magnetic resonance imaging early after chemoradiotherapy to monitor treatment response in head-and-neck squamous cell carcinoma. Int. J. Radiat. Oncol. Biol. Phys. 2012; 82(3): 1098–1107.
219. Kato H, Kanematsu M, Tanaka O, Mizuta K, Aoki M, Shibata T, Yamashita T, Hirose Y, Hoshi H. Head and neck squamous cell carcinoma: usefulness of diffusion-weighted MR imaging in the prediction of a neoadjuvant therapeutic effect. Eur. Radiol. 2009; 19(1): 103–109.
220. Kim S, Loevner L, Quon H, Sherman E, Weinstein G, Kilger A, Poptani H. Diffusion-weighted magnetic resonance imaging for predicting and detecting early response to chemoradiation therapy of squamous cell carcinomas of the head and neck. Clin. Cancer Res. 2009; 15(3): 986–994.